CHAPTER 1

INTRODUCTION

1.1 BACKGROUND OF STUDY

In the early stages of space exploration, when space craft were still small in size, mechanically simple, and almost inflexible, the elastic deformation was meaningless. Now, it is expected that in the future, larger spacecraft will be placed in orbit. The advance of space transportation system makes it possible to consider very large satellites and spacecraft which could be carried into space and deployed, assembled or constructed for such variety of purposes such as communications, astronomy, space exploration and electric power generation. As for example, the Canadian Communication Technology Satellite (CTS) carries two solar panels 1.2m X 7.3m, to generate 1.2kW electric power. [1]

Many of the research before have considered the satellite system to be rigid bodies. When dealing with rigid bodies vibration problem was not so critical. Modern spacecraft, including satellites, consists of structural subsystems, some essentially rigid, such as the rigid main body of satellite, some flexible, such as solar arrays, antennas, and so on. Due to mass limitation, these space vehicles will be extremely flexible. For satellites carrying lightweight deployable members, we cannot assume that there are no elastic deformations. With spacecraft increasing in size and flexibility, the vibration problem of space structures became progressively troublesome. For a flexible space structure, the attitude of main body and the deformations of one flexible member will influence upon the deformations of other flexible members. In the same way, the deformations of flexible members will influence upon the attitude of the whole body of satellite. [2]

1.2 PROBLEM STATEMENT

Attitude maneuvers of flexible satellite using time optimal thrusters may induce large vibration that may cause disturbance to the orientation of the satellite. The large vibration of flexible members cannot be neglected because it can occur easily in maneuvers that finally disturb the pointing of the satellite.

1.3 OBJECTIVE

The purpose of this research is **to implement thrusters based on proportional-derivative (PD) controller for controlling attitude maneuvers of a precise-oriented satellite with flexible solar panels.** Torque inputs working to the satellites are resulted by on-off thrusters, which mean that the satellite will be maneuvered with the constant-amplitude torque commands.

1.4 SCOPE OF STUDY

 – Study of derivation of mathematical model equation of motion of spacecraft with flexible appendages
 – MATLAB simulation of Bang–Bang control by employing the finite element method to discretize the elastic motion of appendages
 – Modify control command of Bang-Bang to PD controller
 – MATLAB simulation of attitude maneuver using PD controller
 – Implement PD controller to thruster mode
 – MATLAB simulation of attitude maneuver using thruster based on PD logic

The particular maneuvers being studied in this project are maneuvers from one rest state to another rest state. It is a fact that in operation the orientation of the satellite must be precise, while the disturbance from the flexible structures may cause errors to the orientation.

CHAPTER 2

LITERATURE REVIEW

2.1 INTRODUCTION

Earlier spacecraft required minimal electrical power since they performed simple missions in space. But the satellites and other space structures today have very complex missions and hence they may need more electrical power. As a result, the solar panels of today's common satellites are required to be large in order to generate sufficient electrical power. [3]

A satellite has to gone through a few stages to fulfill its objective. To understand the stages of these stages will help in over viewing the control system of a satellite. A satellite's life begins with the specific booster transferring it to some initial orbit, called a transfer orbit, in which the satellite is already circling the earth. For a satellite that will stay near earth, the next stage will be to "ameliorate" the orbit; this means that the satellite must be maneuvered to reach precise orbit for which the satellite was designed to fulfill its mission. Next, the satellite's software must check for the proper functioning of its instrumentation and its performance in space, as well as calibrate some of the instruments before they can be used to control the satellite. The final stage is the one for which the satellite was designed and manufactured. [4] In these stages, methods of maneuvering the space craft play a major role to accomplish its mission.

A spacecraft or a satellite in operation needs certain accuracy in its attitude. The KOREASAT requires a satellite with an antenna beam pointing error not greater than $0.07°$ in roll and pitch, and not more than $0.2°$ in yaw [5]. With this criterion, the flexible satellite maneuvered by PD controller must have residual attitude oscillation that is not over the permissible maximum error.

2.2 BANG-BANG COMMAND CONTROL

In control theory, a bang–bang controller (on–off controller), also known as a hysteresis controller, is a feedback controller that switches abruptly between two states. A bang-bang controller operates between two control limits, usually full ON and completely OFF. It can still be a proportional controller if it controls the duty cycle of the ON time versus the OFF time. These controllers may be realized in terms of any element that provides hysteresis.

Due to the discontinuous control signal, systems that include bang–bang controllers are variable structure systems, and bang–bang controllers are thus variable structure controllers. Many researches have been done on control using Bang-bang controller. An investigation was done to control the vibration suppression of flexible spacecraft [6]. The Bang-bang control is simple in formulation, but results in excessive thruster action. Its discontinuous control actions may interact with the flexible modes of spacecraft and result in limit cycles.

Other researchers studied the use of constant-amplitude input to suppress the vibration of the satellite after maneuver. [7] In their words, they applied the method called by input shaping to form the input given to the system.

2.3 PD COMMAND CONTROL

A proportional–integral–derivative controller (PID controller) is a control loop feedback controller widely used in industrial control systems – a PID is the most commonly used feedback controller. However, for best performance, the PID parameters used in the calculation must be tuned according to the nature of the system – while the design is generic, the parameters depend on the specific system. The PID controller calculation (algorithm) involves three separate parameters, and is accordingly sometimes called three-term control: the proportional, the integral and derivative values, denoted P, I, and D.

A proportional controller will have the effect of reducing the rise time and will reduce, but never eliminate, the steady-state error. An integral controller will have the effect of eliminating the steady-state error, but it may make the transient response worse. A derivative controller will have the effect of increasing the stability of the system, reducing the overshoot, and improving the transient response. A PID controller will be called a PI, PD, P or I controller in the absence of the respective control actions. In this study, PD will be used.

Satellite nominal attitude control dynamics is an example of non-linear system where conventional control has been applied successfully since the early space age. PID (proportional-integral-derivative controller) control is commonly used in most satellite attitude control system. This is due to the fact that PID is effective, simple for implementation, and robust against system's uncertainties. [8] However, conventional control like the PD (proportional and derivative of the error) can only guarantee robustness to work in a small region around the reference or nominal attitude. This certainly is not the case of an attitude acquisition, where large maneuvers are commanded autonomously in order to point the satellite close to a nominal attitude. [9]

CHAPTER 3

METHODOLOGY

3.1 RESEACRH METHODOLOGY

Through out this project, research would be done along side with the simulation. This is because apart form grasping the basic knowledge on this topic, the results can also be compared thoroughly with the theories form the research done. The content of the research are planned below:

- Mathematical formulation used on flexible satellite dynamics
- Bang-Bang command control in attitude maneuvering
- Proportional-Derivative (PD) controller in attitude maneuvering
- Interpretations of simulation data

3.2 PROJECT ACTIVITIES FOR FINAL YEAR PROJECT PART 1

In Final Year Project (FYP) part 1, the essential work to do is the research on the background of the project. The studies are more focused on the mathematical model of the spacecraft. Mathematical model in this paper is used based on S. Parman's research [2]. Below are the summarized work done during FYP PART 1:
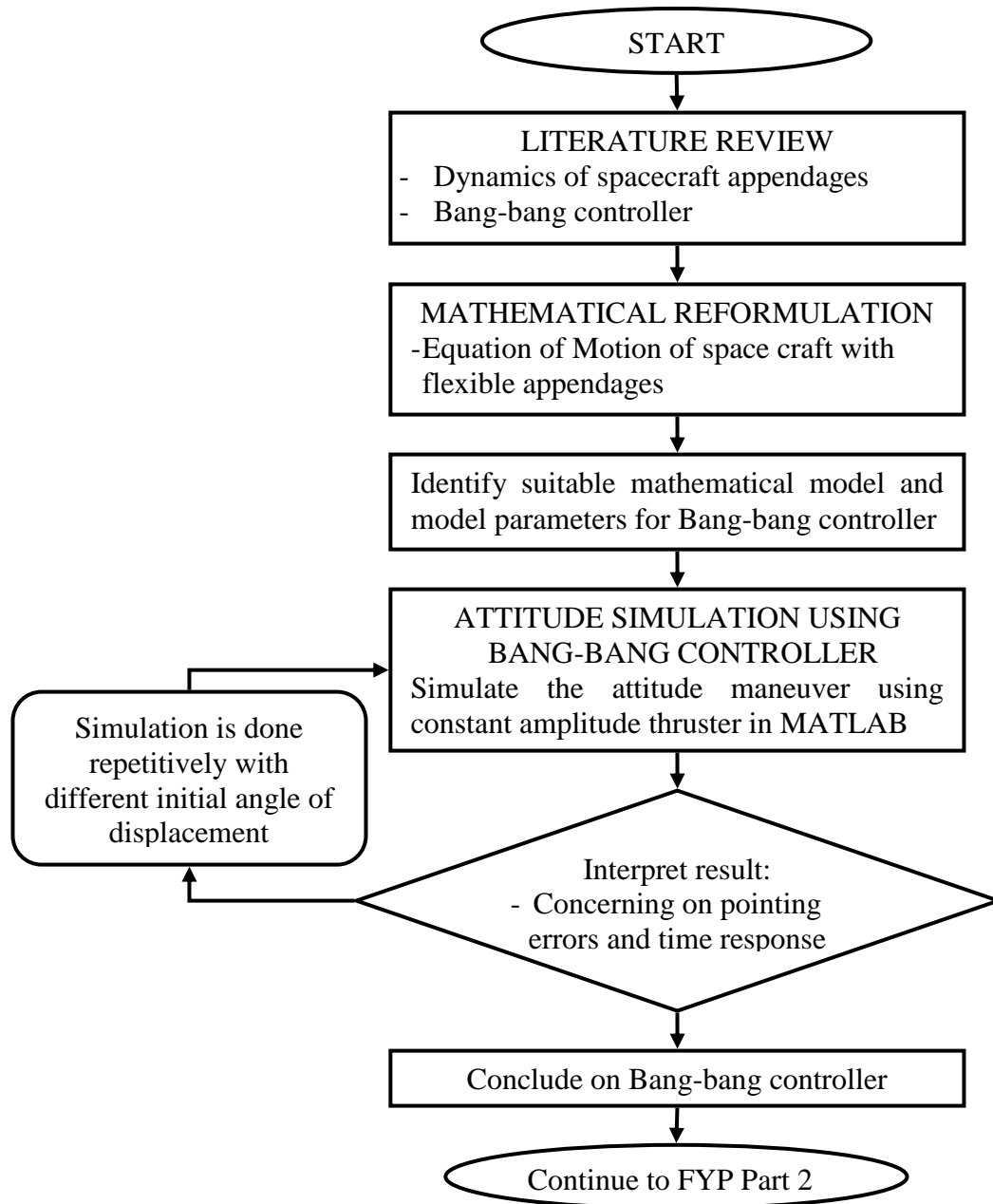
```
                          ┌──────────────┐
                          │    START     │
                          └──────┬───────┘
                                 ▼
              ┌──────────────────────────────────────┐
              │         LITERATURE REVIEW            │
              │  -  Dynamics of spacecraft appendages│
              │  -  Bang-bang controller             │
              └──────────────────┬───────────────────┘
                                 ▼
              ┌──────────────────────────────────────┐
              │    MATHEMATICAL REFORMULATION        │
              │  -Equation of Motion of space craft with │
              │    flexible appendages               │
              └──────────────────┬───────────────────┘
                                 ▼
              ┌──────────────────────────────────────┐
              │ Identify suitable mathematical model and │
              │ model parameters for Bang-bang controller │
              └──────────────────┬───────────────────┘
                                 ▼
              ┌──────────────────────────────────────┐
              │    ATTITUDE SIMULATION USING         │
              │     BANG-BANG CONTROLLER             │
              │  Simulate the attitude maneuver using │
              │  constant amplitude thruster in MATLAB│
              └──────────────────┬───────────────────┘
```

Simulation is done repetitively with different initial angle of displacement

Interpret result:
- Concerning on pointing errors and time response

Conclude on Bang-bang controller

Continue to FYP Part 2

Figure 1 Flow chart of FYP Part 1

3.3 PROJECT ACTIVITIES FOR FINAL YEAR PROJECT PART 2

Project activities for Final Year Project Part 2 (FYP 2), has been successfully completed in the planned time range. In this part, the focus is moved to the attitude maneuvering using PD controller. Basically, the flow chart of using PD controller is as below in figure 2:
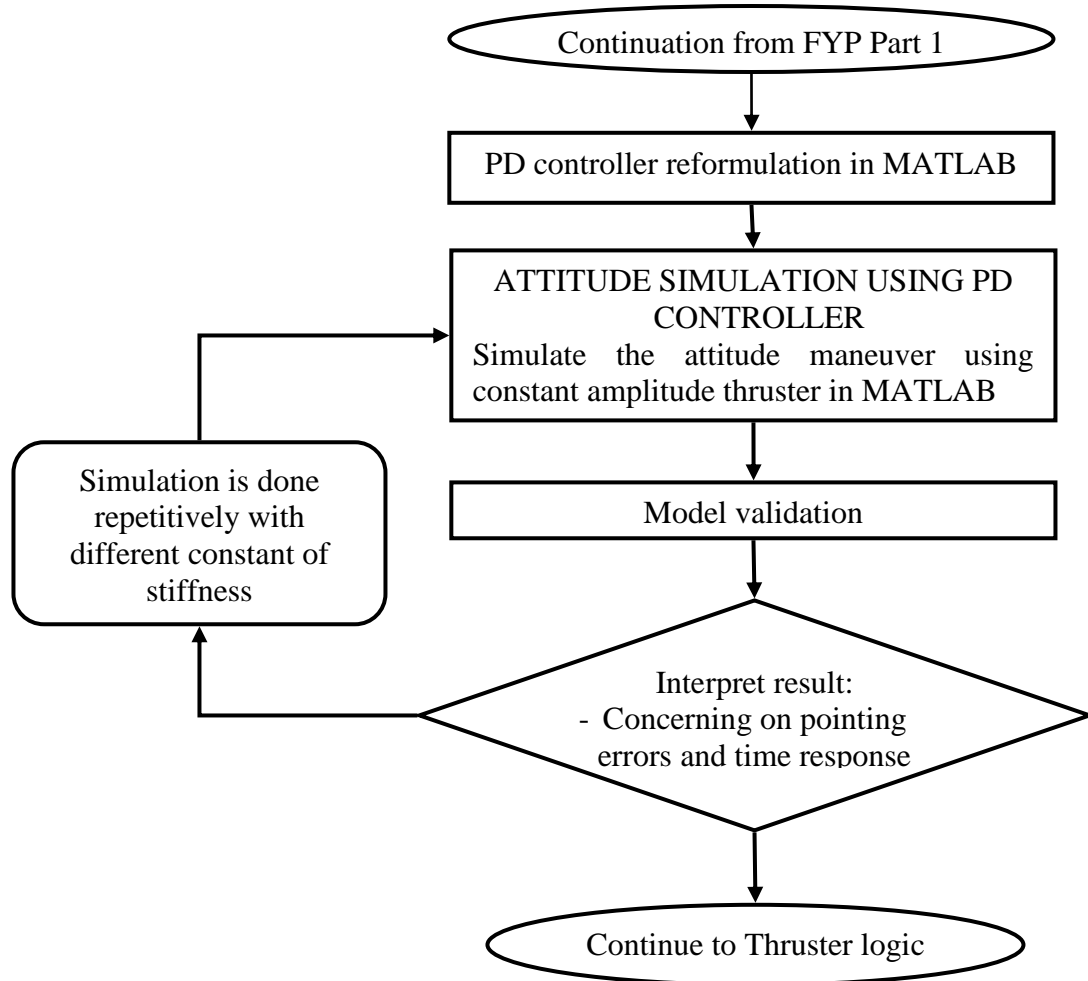
```
                    ┌──────────────────────────────┐
                    │  Continuation from FYP Part 1 │
                    └──────────────────────────────┘
                                   │
                                   ▼
                    ┌──────────────────────────────┐
                    │ PD controller reformulation   │
                    │ in MATLAB                      │
                    └──────────────────────────────┘
                                   │
                                   ▼
                    ┌──────────────────────────────┐
                    │  ATTITUDE SIMULATION USING PD │
                    │          CONTROLLER            │
                    │ Simulate the attitude maneuver │
                    │ using constant amplitude       │
                    │ thruster in MATLAB             │
                    └──────────────────────────────┘
                                   │
    ┌────────────────┐             ▼
    │ Simulation is  │  ┌──────────────────────────────┐
    │ done           │  │       Model validation        │
    │ repetitively   │  └──────────────────────────────┘
    │ with different │             │
    │ constant of    │             ▼
    │ stiffness      │       ◇ Interpret result:
    └────────────────┘       - Concerning on pointing
                               errors and time response ◇
                                   │
                                   ▼
                    ┌──────────────────────────────┐
                    │  Continue to Thruster logic   │
                    └──────────────────────────────┘
```

Figure 2 : Flow chat of PD simulation in FYP part 2

The control command for the maneuvering is reformulate again into PD controller. Then, Simulation is done on PD controller and the result is interpreted. The simulation is done repetitively using different stiffness constant to choose the best result. After the desired result was chosen, thruster logic was defined based on that PD.

```
        ┌─────────────────────────────────────┐
        │    Continuation from PD controller   │
        └─────────────────────────────────────┘
                        │
                        ▼
        ┌─────────────────────────────────────┐
        │   Thruster logic definition based on PD
        │              controller              │
        └─────────────────────────────────────┘
                        │
                        ▼
        ┌─────────────────────────────────────┐
        │    ATTITUDE SIMULATION OF LOGIC      │
        │   THRUSTERS BASED ON PD CONTROL      │
        │ Simulate the attitude maneuver in MATLAB │
        └─────────────────────────────────────┘
                        │
                        ▼
        ┌─────────────────────────────────────┐
        │           Model validation          │
        └─────────────────────────────────────┘
                        │
                        ▼
        ┌─────────────────────────────────────┐
        │            Interpret result:         │
        │ Concerning on pointing errors and time response │
        └─────────────────────────────────────┘
                        │
                        ▼
        ┌─────────────────────────────────────┐
        │  Comparing 3 modes of control; Bang-bang
        │  command control, PD controller, and thruster
        │  logic based on PD control           │
        └─────────────────────────────────────┘
                        │
                        ▼
        ┌─────────────────────────────────────┐
        │   Overall interpretation of the results │
        └─────────────────────────────────────┘
                        │
                        ▼
        ┌─────────────────────────────────────┐
        │    Discussions and recommendation    │
        └─────────────────────────────────────┘
                        │
                        ▼
        ┌─────────────────────────────────────┐
        │             Conclusion               │
        └─────────────────────────────────────┘
```

Figure 3 Flow chart of implementing thrusters based on PD controller

According to figure 3, thruster logic is first defined based on PD controller. Then, it is simulated and the result is interpreted. After all the three modes of controller are simulated, the result is then compared and analyzed. The results are discussed and recommendations are given. Lastly, the project was concluded.

3.4 GANTT CHART

The schedules and milestone for this project (including FYP 1 and FYP 2) is provided in the **appendix 1.**

3.5 TOOLS REQUIRED

- **MATLAB 7.1** will be used throughout this project.

CHAPTER 4

RESULTS AND DISCUSSION

To accomplish this project, researches must be done. The basic of this modeling project is the equation of motion of the flexible satellite. Thus, to carry out this project in the limited time frame, the equation of motion was studied and referred to. Most of the modeling is based on S. Parman's research [2]. The summaries of findings are;

4.1 EQUATIONS OF MOTION OF A SPACE CRAFT WITH FLEXIBLE APPENDAGES

Researchers have done a lot of modeling a spacecraft carrying flexible substructures mathematically. Recently, considerable attention has been devoted to the problem of modeling and control of large structures. Flexibility of various components introduces additional complexities in control and stabilization of the spacecraft. In order to study the effects of structural flexibility on the motion system, it is necessary to develop a model that is mathematically rigorous and yet simple enough for theoretical as well as numerical investigation [4]. Generally, there are three alternative approaches to make the mathematical model. The first approach: the substructures are idealized as collections of small rigid bodies interconnected by mass less elastic structures [10]. The second approach: the substructures are treated as elastic continua [11]. Then, the third approach: the substructures are modeled as collections of finite elements possessing mass, interconnected at nodes, where masses may or may not be concentrated. The third approach demonstrated features which the resulting dynamical formulation especially in observing the three-dimensional motion of spacecraft having a lot of nodes [12].

In this project, the third approach will be used for the mathematical formulation of flexible spacecraft dynamics, which is the finite element approach. The spacecraft

consist of two main parts which is the main body (rigid body) and the flexible substructures. The flexible substructures are in the form of solar panels, antennas, booms and etc. The first was to determine coordinate reference frames to measure the attitude motion of the rigid body and displacements of the flexible components. The equation of motion of the space craft was developed by using Lagrange's formulation. So, kinetic and potential energies must be expressed first. The orientation angles of the spacecraft, and system rotations were expressed in Bryant equation. As the discrete coordinates used in that study, it will be introduced the *inertial reference frame*, *orbital reference frame*, and *rigid main body-fixed reference frame*; while the distributed coordinates, the *flexible substructure local reference frames* will be defined.

4.1.1 Coordinate Reference Frame

A typical modern spacecraft consist of structural subsystems, some essentially rigid and other are extremely flexible, interconnected often in a time-varying manner, with relative motions frequently prescribed by nonlinear automatic control systems. Such vehicles may in whole or in part be spinning. The vehicles are expected to undergo arbitrary large changes in inertial orientation and they may also be subjected to external forces due to environmental interaction and due to the actuation of attitude control devices. Hybrid coordinate approach should be used to analyze the dynamic of the vehicle. The analysis should combine the generalities of nonlinearity and unrestricted motions provided by the representation of vehicle as a collection of interconnected discrete rigid bodies. The hybrid coordinate approach combines discrete coordinates describing the translations and rotations of some bodies or reference frames of the system with distributed or modal coordinates describing the small relative motions of other parts of the system. This approach is illustrated by application to a simplified spinning spacecraft system. The example illustrates many features of flexural systems engaged in spin.

Hybrid system of reference frames will:
  i.   Simplify the expression of potential energy and kinetic energy
  ii.   Simplify the formulation of equation of motion

iii. Simplify the constraint equations relating to the orientation of the frame relative to the structure

iv. Able to separate equations governing the spacecraft's rigid body motion from the motion of elastic deformations of flexible structures

Inertial Reference Frame, $F_i(O_i x_i y_i z_i)$

All spacecraft motions will refer to Inertial Reference Frame, $F_i(O_i X_i Y_i Z_i)$. Its coordinate system is fixed with respect to stars. However, the inertial reference frame is a reference coordinate set which guarantees the required accuracy over the time interval of interest. In this study, because of the time intervals of observations are short enough compared to the orbit period, the origin of the reference frame, O_i, is selected at a point of the nominal orbit of the spacecraft in the undeformed state. One axis (X_i) is directed along a fixed celestial direction in the orbit plane, another axis (Y_i) is normal to the orbit plane, and the third axis (Z_i) completes the orthogonal set using the right-hand-side law. The inertial reference frame is presented by unit vectors $\mathbf{i}_i$, $\mathbf{j}_j$, $\mathbf{k}_i$ as shown in Figure 4. The $\mathbf{i}_i$ is the unit vector in the X_i-direction, $\mathbf{j}_j$ is the unit vector in the Y_i– direction, and $\mathbf{k}_i$ is the unit vector in the Z_i–direction.
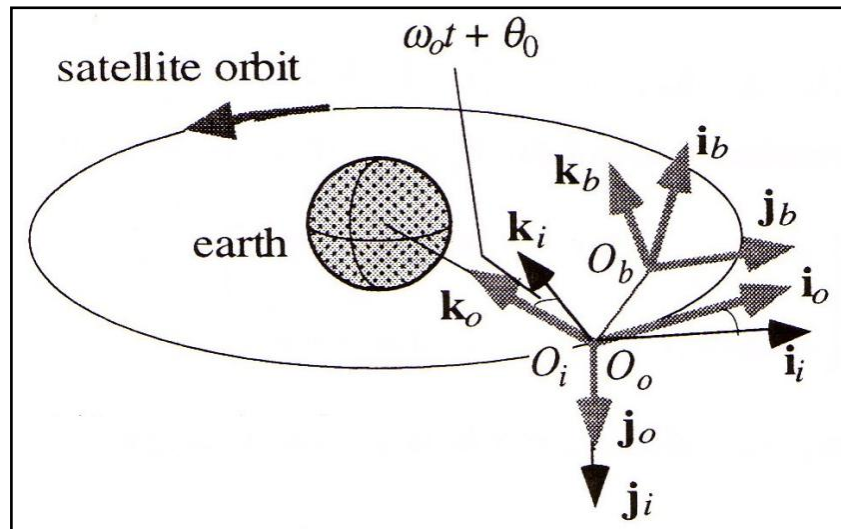
Figure 4 The inertial reference frame F_i, the orbital reference frame F_o, and the body fixed reference frame F_b definitions

<u>Orbital reference frame,</u> $F_o (O_O X_o Y_o Z_o)$

Orbital reference frame $F_o (O_O X_o Y_o Z_o)$ is presented by unit vectors $\mathbf{i}_o$, $\mathbf{j}_o$ and $\mathbf{k}_o$; where $\mathbf{i}_o$, $\mathbf{j}_o$ and $\mathbf{k}_o$ are the unit vectors in the X_o, Y_o, and Z_o –directions respectively. Refer to figure 4, the origin of the orbital reference frame O_o is located on the nominal spacecraft orbit, X_o-axis points to the orbital direction, Z_o-axis points to the center of the earth, Y_o – axis completes the orthogonal system (normal to the orbit plane) by using the right-hand-side law. Based on figure 4, the transformation of a vector in the inertial reference frame F_i to the orbital reference frame F_o can be expressed as

$$\{\mathbf{i}o \ \mathbf{j}o \ \mathbf{k}o\}^T = \mathbf{T}_{i,o} \{\mathbf{i}i \ \mathbf{j}i \ \mathbf{k}i\}^T \qquad (4.1)$$

where $\mathbf{T}_{i,o}$ is the transformation matrix from F_i to F_o, that can be written as follows:

$$\mathbf{T}_{i,o} = \begin{bmatrix} \cos{(\omega o t + \theta o)} & 0 & \sin{(\omega o t + \theta o)} \\ 0 & 1 & 0 \\ -\sin{(\omega o t + \theta o)} & 0 & -\cos{(\omega o t + \theta o)} \end{bmatrix} \qquad (4.2)$$

where ω_o is the orbital angular velocity, and θ_o is a constant angle.

<u>Rigid main body fixed reference frame,</u> $F_b (O_b X_b Y_b Z_b)$

Rigid main body fixed reference frame, $F_b (O_b X_b Y_b Z_b)$, is represented by the unit vector $\mathbf{i}_b$, $\mathbf{j}_b$ and $\mathbf{k}_b$, with the origin O_b. The $\mathbf{i}_b$ is the unit vector in the X_b-direction, $\mathbf{j}_b$ is the unit vector in the Y_b- direction, and $\mathbf{k}_b$ is the unit vector in the Z_b-direction. This reference frame is assumed to fix to the rigid main body of spacecraft. It can be selected to coincide the mass centre of the whole spacecraft, but it may also be selected to be different with the mass centre of spacecraft. The orientation of the rigid main body fixed reference frame could be arbitrary in space. In order to observe the attitude of spacecraft, the orientation of this reference frame with respect to the inertial reference frame must be known. The transformation of a vector in the orbital reference frame F_o to the rigid main body fixed reference frame F_b can be written as

15

$$\{\mathbf{i_b}\ \mathbf{j_b}\ \mathbf{k_b}\}^T = \mathbf{T}_{o,b}\{\mathbf{i_o}\ \mathbf{j_o}\ \mathbf{k_o}\}^T \tag{4.3}$$

where $\mathbf{T}_{o,b}$ is the transformation matrix from F_o to F_b, and the matrix $\mathbf{T}_{o,b}$ is given by

$$\mathbf{T}_{o,b} = \begin{bmatrix} c\theta c\psi & c\theta s\psi & -s\theta \\ s\phi s\theta c\psi + c\phi s\psi & s\phi s\theta s\psi + c\phi c\psi & s\phi c\theta \\ c\phi s\theta c\psi + s\phi s\psi & c\phi s\theta s\psi - s\phi c\psi & c\phi c\theta \end{bmatrix} \tag{4.4}$$

"s" and *"c"* in equation 4.4 express the sine and cosine functions respectively. If the Bryant angles are small, the transformation matrix $\mathbf{T}_{o,b}$ can be simplified as follows:

$$\mathbf{T}_{o,b} = \begin{bmatrix} 1 & \psi & -\theta \\ -\psi & 1 & \phi \\ \theta & -\phi & 1 \end{bmatrix} \tag{4.5}$$

The transformation from the inertial reference frame to the rigid main body fixed reference frame will be found by substituting equation 4.1 in 4.3. The transformation of the vector expressed in F_i to the same vector expressed in F_b can be written as follows:

$$\{\mathbf{i_b}\ \mathbf{j_b}\ \mathbf{k_b}\}^T = \mathbf{T}_{o,b,}\ \mathbf{T}_{i,o}\{\mathbf{i_i}\ \mathbf{j_i}\ \mathbf{k_i}\}^T \tag{4.6}$$

Flexible substructure local reference frame, $F_l\ (O_lX_lY_lZ_l)$

Equation of motion of flexible substructures of spacecraft is developed by flexible substructure local reference frame $F_l\ (O_lX_lY_lZ_l)$. It is represented by the unit vectors $\mathbf{i_l}$, $\mathbf{j_l}$ and $\mathbf{k_l}$. The $\mathbf{i_l}$ is the unit vector in X_l-direction, $\mathbf{j_l}$ is the unit vector in the Y_l-direction and $\mathbf{k_l}$ is the unit vector in the Z_l-direction. For any flexible substructures, the origin Ol is fixed at a certain position in the substructure, and the unit vectors $\mathbf{i_l}$, $\mathbf{j_l}$, and $\mathbf{k_l}$ point to suitable directions, that causes the expression of its elastic deformations to be simple. The definition of the local reference frame can be seen in figure 5.
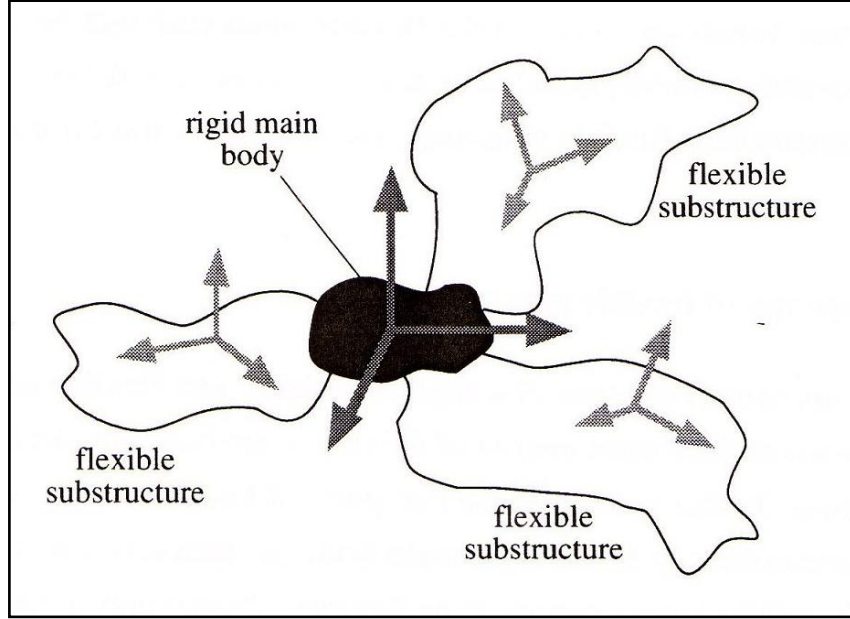
Figure 5 The flexible substructure local reference frame F_l definition

The transformation of a vector expressed in F_b to the same vector expressed in F_l can be written as follows:

$$\{\mathbf{i}_l \, \mathbf{j}_l \, \mathbf{k}_l\}^T = \mathbf{T}_{b,l}\{\mathbf{i}_b \, \mathbf{j}_b \, \mathbf{k}_b\}^T \qquad (4.7)$$

where $\mathbf{T}_{b,l}$ denotes a transformation matrix from F_b to F_l.

According to this paper, the finite element method was applied to analyze the elastic motion of flexible substructures of space craft [2]. Thus, the flexible substructures are divided into a number of elements. Each element has its own reference frame. It means that the number of flexible substructure local reference frame is as same as the number of substructure's elements. The flexible substructure local reference frame is located in each discussed element. The orientation of the reference frame for one element is permitted to differ with the reference frame for other element.

4.1.2 The Mathematical Modeling of Flexible Spacecraft Dynamics

Based on S. Parman paper, equation of motion is derived using a Lagrangian and Lagrange's equation of motion [2]. Kinetic and potential energy of the flexible spacecraft is defined first. Lagrangian can be formulated by defining those energies. Then, the Lagrangian is employed in the Lagrange's equation of motion. The kinetic energy of the spacecraft will consist of kinetic energy of the main body and the kinetic energy of the flexible substructures.

Kinetic energy of flexible spacecraft

Consider a particle p with mass dm in the rigid body, as shown in figure 6. The kinetic energy of the particle relative to the inertial reference frame can be written as;

$$dE_{kb} = \frac{1}{2}\, \dot{\mathbf{r}}_{i,p}^{T}\, \dot{\mathbf{r}}_{i,p}\, dm \tag{4.8}$$

where dE_{kb} is the kinetic energy of the particle, and $\mathbf{r}_{i,p}$ is a vector from the inertial reference frame F_i to the discussed particle p, and the "dot" means the differentiation with respect to time. The vector $\mathbf{r}_{i,p}$ of the rigid main body is composed by

$$\mathbf{r}_{i,p} = \mathbf{r}_{i,b} + \mathbf{r}_{b,p} \tag{4.9}$$

where $\mathbf{r}_{i,b}$ is a vector from the origin of the inertial reference frame, O_i, to the origin of the main body-fixed reference frame, O_b; and $\mathbf{r}_{b,p}$ is a vector from O_b to the discussed particle p.
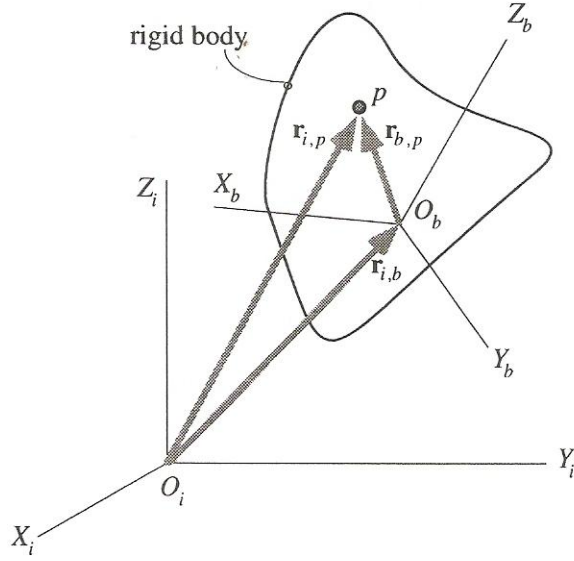
Figure 6 Representation of $r_{b,p}$ in the body fixed reference frame F_b

Since F_b is moving relative to F_i, the differentiation of $\mathbf{r}_{b,p}$ with respect to time relative to F_i can be written as

$$\dot{\mathbf{r}}_{b,p} = {}^b\dot{\mathbf{r}}_{b,p} + \boldsymbol{\omega}_{b,i} \times {}^b\mathbf{r}_{b,p} \tag{4.10}$$

where ${}^b\mathbf{r}_{b,p}$ means the differentiation of $\mathbf{r}_{b,p}$ with respect to time, measured in F_b; ${}^b\mathbf{r}_{b,p}$ is $\mathbf{r}_{b,p}$ presented in F_b; and $\omega_{b,i}$ is the angular velocity of F_b relative to F_i.

For the kinetic energy of the rigid body of spacecraft, the author obtains:

$$\mathrm{E_{kb}} = \frac{1}{2}\dot{\boldsymbol{r}}_{i,b}^T\dot{\boldsymbol{r}}_{i,b}m_b + \frac{1}{2}\boldsymbol{\omega}_{b,i}^T\mathbf{I}_b\boldsymbol{\omega}_{b,i} + \dot{\boldsymbol{r}}_{i,b}^T\boldsymbol{Q}_b\boldsymbol{\omega}_{b,i} \tag{4.11}$$

where m_b is the total mass of the rigid main body. $\mathbf{Q}_b$ can be expressed in the form:

$$\mathbf{Q}_b = \begin{bmatrix} 0 & Q_z & -Q_y \\ -Q_z & 0 & Q_x \\ Q_y & -Q_x & 0 \end{bmatrix} \tag{4.12}$$

The inertia matrix relative to O_b:

$$\mathbf{I}_b = \int_{\mathrm{mb}} {}^b\tilde{\boldsymbol{r}}_{b,p}^T \, {}^b\tilde{\boldsymbol{r}}_{b,p} \, dm \tag{4.13}$$

19

$$\mathbf{I}_b = \begin{bmatrix} I_x & -I_{xy} & -I_{xz} \\ -I_{xy} & I_y & -I_{yz} \\ -I_{xz} & -I_{yz} & I_z \end{bmatrix} \tag{4.14}$$

The kinetic energy of flexible substructures

In this analysis, the kinetic energy of flexible substructures has obtained from the case where the rigid main body of the space craft was allowed to execute translational and rotational motions. The kinetic energy of flexible substructures has been derived using the finite element method. As the first step in the finite element method, the flexible substructures are replaced by a finite collection on *N* structural elements. Each element is idealized as an elastic body. One element connects with its neighbor elements at discrete contact points. Each contact point is called a node.

Each element should have its own reference frame to analyze its deformation. It means that flexible substructure local reference frames, F_l *(l=1, 2,…,N)*, need to be defined. The local reference frame should be chosen in a suitable form for the simplicity of analysis. Consider a particle *p* in the flexible substructure with mass *dm* as shown in Figure 7. Its kinetic energy can be written as follows:

$$dE_{ka} = \frac{1}{2} \dot{\mathbf{R}}_{i,p}^T \, \dot{\mathbf{R}}_{i,p} \; dm \tag{4.15}$$

where dE_{ka} is the kinetic energy of the discussed particle, and $\mathbf{R}_{i,p}$ is a vector form the origin of the inertial reference frame, $\mathbf{O}_i$, to the discussed particle *p,* while the " $\dot{}$ " means the differentiation with respect to time.

By seeing Figure 7, the vector $\mathbf{R}_{i,p}$ can be composed as:

$$\mathbf{R}i,p = \mathbf{r}\, i,b + \mathbf{R}_{b,o} + \mathbf{R}_{o,p0} + \mathbf{R}_{p0,p} \tag{4.16}$$

20

where $\mathbf{R}_{b,o}$ is the vector form O_b to O_l ; $\mathbf{R}_{o,po}$ is the vector form O_l to any undeformed particle position p_0 ; $\mathbf{R}_{p0,p}$ is the vector form p_o to the corresponding deformed particle position p. The vector $\mathbf{R}_{p0,p}$ will then be called the deformation vector.
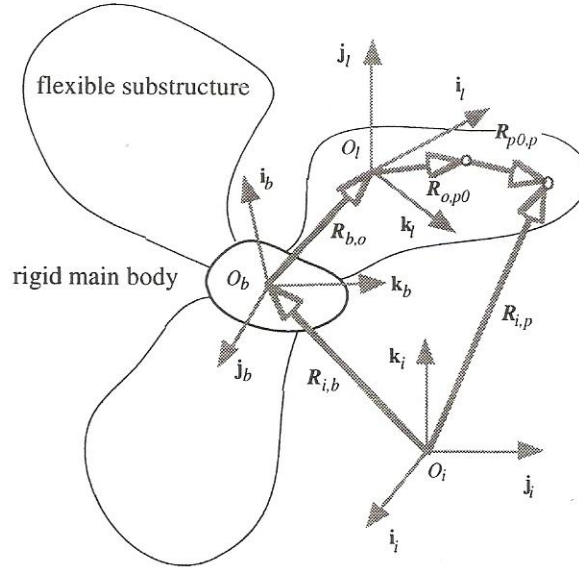
Figure 7 The example of a flexible substructure local reference frame F_l

The local reference frame of F_l may be moving relative to the body fixed reference frame F_b, if the flexible substructure is allowed to have one or more kinematic degrees of freedom relative to the spacecraft rigid main body. For example, the spacecraft rigid main body may be desired pointing to the centre of the earth while the flexible solar panels have to be oriented towards the sun. Therefore, the transformation matrix from F_b to F_l, $\mathbf{T}_{b,l}$ is a time varying matrix in general. However, it is assumed that is variation is sufficiently show to allow a *quasi-stationary* (i.e. time constant) approximation of the transformation matrix $\mathbf{T}_{b,l}$ for relatively short time intervals. This approximation is reasonable when the period of the slowest flexible structure motion is much shorter than the orbital period.

Taken $\mathbf{R}_{b,o}$ and $\mathbf{R}_{b,p0}$ are constant vectors in the local reference frame, or

$$^{l}\mathbf{R}_{b,o} = \; ^{l}\dot{\mathbf{R}}_{b,o} = 0 \tag{4.17}$$

and only small deformations of flexible substructures are considered, so $^{l}\mathbf{R}_{b,o} + \; ^{l}\mathbf{R}_{b,p0} +$ $^{l}\mathbf{R}_{p0,p} = \; ^{l}\mathbf{R}_{b,o} + \; ^{l}\mathbf{R}_{o,p0.}$ The equivalent matrix form of the differentiation of equation (4.15) with respect to time in the inertial reference frame is

$$dE_{ka} = \frac{1}{2} \{ \; \dot{\mathbf{r}}_{i,b}^{T} \; \dot{\mathbf{r}}_{i,b} + \; ^{l}\dot{\mathbf{R}}_{p0,p}^{T} \quad ^{l}\dot{\mathbf{R}}_{p0,p} + \boldsymbol{\omega}_{b,i}^{T} \; \mathbf{T}_{b,l}^{T} (\; ^{l}\widetilde{\mathbf{R}}_{b,o} + \; ^{l}\widetilde{\mathbf{R}}_{o,p0})^{T} (\; ^{l}\widetilde{\mathbf{R}}_{b,o} + \; ^{l}\widetilde{\mathbf{R}}_{o,p0})$$

$$\mathbf{T}_{b,l} \, \omega_{b,i} + 2 \, \boldsymbol{\omega}_{b,i}^{T} \; \mathbf{T}_{b,l}^{T} (\; ^{l}\widetilde{\mathbf{R}}_{b,o} + \; ^{l}\widetilde{\mathbf{R}}_{o,p0}) \; ^{l}\dot{\mathbf{R}}_{p0,p} + 2 \, \dot{\mathbf{r}}_{i,b}^{T} \; \mathbf{T}_{b,l}^{T} (\; ^{l}\widetilde{\mathbf{R}}_{b,o} + \; ^{l}\widetilde{\mathbf{R}}_{o,p0})^{T}$$

$$\mathbf{T}_{b,l} \, \omega_{b,i} + 2 \, \dot{\mathbf{r}}_{i,b}^{T} \; \mathbf{T}_{b,l}^{T} \{ \; ^{l}\dot{\mathbf{R}}_{p0,p} \} \, dm$$

$$(4.18)$$

The kinetic energy of the discussed element is obtained by integrating equation (4.18) within one element, i.e;

$$\mathrm{E}_{kai} = \int_{Ei} dE_{ka} \tag{4.19}$$

It should be noted that the symbol $\int_{Ei}$ means integrations within the whole element i and the mass of element $i,$ respectively. Because the flexible substructures contain N elements, the total kinetic energy of the flexible substructures is

$$\mathrm{E}_{ka} = \sum_{i=1}^{n} E_{kai} \tag{4.20}$$

where E_{kai} is the kinetic energy of the ith element.

Equation E_{kai} obtained can be written as below by using equation (4.20), (4.21), (4.22), and (4.23);

22

$$E_{kai} = \frac{1}{2}\,\dot{\mathbf{r}}_{i,b}^{T}\dot{\mathbf{r}}_{i,b}m_i + \frac{1}{2}\,\dot{\mathbf{d}}_i^{T}\mathbf{M}_i\,\dot{\mathbf{d}}_i + \frac{1}{2}\,\boldsymbol{\omega}_{b,i}^{T}\,\mathbf{T}_{b,l}^{T}\,\mathbf{I}_i\,T_{b,l}\,\omega_{b,i} + \boldsymbol{\omega}_{b,i}^{T}\mathbf{T}_{b,l}^{T}\,\mathbf{A}_i\dot{\mathbf{d}}_i + \dot{\mathbf{r}}_{i,b}^{T}\mathbf{T}_{b,l}^{T}\,\mathbf{Q}_i\,\mathbf{T}_{b,l}$$
$$\omega_{b,i} \quad + \;\dot{\mathbf{r}}_{i,b}^{T}\mathbf{T}_{b,l}^{T}\,\mathbf{W}_i\dot{\mathbf{d}}_i \tag{4.21}$$

$\mathbf{M}_i$ is called the total mass matrix with respect to all nodal displacements of the ith element.

$$\mathbf{M}_i = \int_{mi} \mathbf{C}_i^{T}\,\mathbf{C}_i \tag{4.22}$$

$$\mathbf{W}_i = \int_{mi} \mathbf{C}_i\,dm \tag{4.23}$$

$$\mathbf{V}_i = \int_{mi}^{l} R_{o,p0}\,\mathbf{C}_i\,dm \tag{4.24}$$

$$\mathbf{A}_i = {}^{l}\widetilde{\mathbf{R}}_{b,o}\,\mathbf{W}_i + \mathbf{V}_i \tag{4.25}$$

If the mass density of the chosen element is uniform, the equation can be written as:

$$\mathbf{I}i = \rho_i\,\mathbf{V}_i\;{}^{l}\widetilde{\mathbf{R}}_{b,o}^{T}\;\;{}^{l}\widetilde{\mathbf{R}}_{b,o} + \mathbf{I}_{Ei} \tag{4.26}$$

where ρ_i is the mass density of the ith element, $\mathbf{V}_i$ is the volume of the ith element, and

$$\mathbf{I}_{Ei} = \rho_i\,[\;{}^{l}\widetilde{\mathbf{R}}_{b,o}^{T}\;\int_{Vi}^{l}\widetilde{\mathbf{R}}_{o,p0}^{T}dV + [\;{}^{l}\widetilde{\mathbf{R}}_{b,o}^{T}\;\int_{Vi}^{l}\widetilde{\mathbf{R}}_{o,p0}^{T}dV]^{T} + \int_{Vi}^{l}\widetilde{\mathbf{R}}_{o,p0}^{T}\;{}^{l}\widetilde{\mathbf{R}}_{o,p0}dV] \tag{4.27}$$

The relation between the ith element displacement vector $\mathbf{d}_i$ and the total flexible substructure displacement vector $\mathbf{d}$ can be written as

$$\mathbf{D}_i = \mathbf{P}_i\mathbf{d} \tag{4.28}$$

where $\mathbf{P}_i$ is called the assembling matrix.

By substituting equation (4.26), (4.27) and equation (4.28), (4.29), (4.30), (4.31), (4.32) and (4.33) into the equation (4.19), will produce the total kinetic energy of flexible substructure in the form of;

$$E_{ka} = \frac{1}{2}\,\dot{\mathbf{r}}_{i,b}^{T}\;\dot{\mathbf{r}}_{i,b}m_a + \frac{1}{2}\,\dot{\mathbf{d}}^{T}\mathbf{M}\,\dot{\mathbf{d}} + \frac{1}{2}\,\boldsymbol{\omega}_{b,i}^{T}\mathbf{A}\dot{\mathbf{d}} + \frac{1}{2}\,\boldsymbol{\omega}_{b,i}^{T}\,\mathbf{I}_a\,\omega_{b,i} + \dot{\mathbf{r}}_{i,b}^{T}\,\mathbf{W}\,\dot{\mathbf{d}} + \dot{\mathbf{r}}_{i,b}^{T}\,\mathbf{Q}_a\,\omega_{b,i}$$
$$\tag{4.29}$$

where ($\frac{1}{2}$ $\dot{\mathbf{r}}_{i,b}^{\mathrm{T}}$ $\dot{\mathbf{r}}_{i,b} m_a$) is the kinetic energy due to the translational displacements of undeformed flexible substructures; ($\frac{1}{2}$ $\dot{\mathbf{d}}^T$ $\mathbf{M}$ $\dot{\mathbf{d}}$) is the kinetic energy due to the deformation of flexible substructures; ($\frac{1}{2}$ $\boldsymbol{\omega}_{b,i}^{T}$ $\mathbf{I}_a$ $\omega_{b,i}$) is the kinetic energy due to the rotational displacements of undeformed flexible substructures; ($\boldsymbol{\omega}_{b,i}^{T} \mathbf{A} \dot{\boldsymbol{d}}$) is the coupling kinetic energy due to rotational displacements of the spacecraft rigid main body and the displacements of deformed flexible substructures; ($\dot{\mathbf{r}}_{i,b}^{\mathrm{T}}$ $\mathbf{W}$ $\dot{\mathbf{d}}$) is the coupling kinetic energy due to translational displacements of the spacecraft rigid main body and the displacements of deformed flexible substructures; and ($\dot{\mathbf{r}}_{i,b}^{\mathrm{T}}$ Q_a $\omega_{b,i}$) is the coupling kinetic energy due to the translational and rotational displacements of the spacecraft main body. It is noted here, that in equation (4.21) to equation (4.29) be presented $\mathbf{T}_i$ instead of $\mathbf{T}_{b,l}$ since it is assumed that the local reference frame could be different for every element.

Define

$$m_a = \sum_{i=1}^{N} m_i \tag{4.30}$$

as a total mass of flexible substructures;

$$\mathbf{M} = \sum_{i=1}^{N} \mathbf{P}_i^{T} \mathbf{M}_i \mathbf{P}_i \tag{4.31}$$

as a total mass matrix of flexible substructures;

$$\mathbf{I}_a = \sum_{i=1}^{N} \mathbf{T}_i^{T} \mathbf{I}_i \mathbf{T}_i \tag{4.32}$$

as a inertia matrix of flexible substructures;

$$\mathbf{A} = \sum_{i=1}^{N} \mathbf{T}_i^{T} \mathbf{A}_i \mathbf{P}_i \tag{4.33}$$

as a total coupling matrix for the rotational displacements of the rigid main body and the flexible substructure displacements;

24

$$W = \sum_{i-1}^{N} \mathbf{T}_i^T \, \mathbf{W}_i \, \mathbf{P}_i \qquad (4.34)$$

as a total coupling matrix for the translational displacements of the rigid main body and the flexible substructure displacements; and

$$\mathbf{Q} = \sum_{i=1}^{N} \mathbf{T_i}^T \, \mathbf{Q}_i \, \mathbf{T}_i \qquad (4.35)$$

as the total coupling matrix for the translational and rotational displacements of the rigid main body.

The total kinetic energy of spacecraft

The total kinetic energy of a flexible spacecraft can be obtained by summing the kinetic energy of a rigid main body and flexible substructures;

$$E_k = E_{kb} + E_{ka} \qquad (4.36)$$

where E_{kb} is the kinetic energy of the rigid main body, and E_{ka} is the kinetic energy of flexible substructures. Substituting equation (4.11) and (4.29) into equation (4.36), it can be written:

$$E_k = \frac{1}{2}\dot{r}_{i,b}^T\dot{r}_{i,b}m_b \ + \frac{1}{2}\omega_{b,i}^T\mathbf{I}_b\omega_{b,i} + \ \frac{1}{2}\dot{\mathbf{d}}^T\mathbf{M}\,\dot{\mathbf{d}} \ + \frac{1}{2}\omega_{b,i}^T\mathbf{A}\dot{d} + \dot{\mathbf{r}}_{i,b}^T\,\mathbf{W}\,\dot{\mathbf{d}} \ +\dot{r}_{i,b}^T\mathbf{Q}_b\omega_{b,i}$$
(4.37)

where $\mathbf{I} = \mathbf{I}_a + \mathbf{I}_b$ is the total inertia matrix of the spacecraft; $m = m_a + m_b$ is the total mass of spacecraft; and $\mathbf{Q} = \mathbf{Q}_a + \mathbf{Q}_b$ is the total coupling matrix between the translational and rotational displacements of an undeformed spacecraft.

Potential energy of a flexible spacecraft

The potential energy of a flexible spacecraft consists of the potential energy of an undeformed spacecraft and the potential energy of deformed flexible substructures.

The potential energy of an undeformed spacecraft

The potential energy of a flexible spacecraft is measured relative to the earth. If $\mathbf{F}r$ is conservative;

$$W = - \int dE_{pr} = -Epr\,(\mathbf{r}) \tag{4.38}$$

where

$$\mathbf{r} = \mathbf{r}_{e,i} + \mathbf{r}_{i,b} \tag{4.39}$$

and $\mathbf{r}_{e,i,}$ a vector from gravity centre of the earth to the origin of the inertial reference frame, is a constant vector expressed in the inertial reference frame, F_i, so

$$E_{pr} = E_{pr}\,(\mathbf{r}_{i,b}) \tag{4.40}$$

The potential energy of an undeformed spacecraft

Became the spacecraft consists of a rigid main body and flexible substructures, so the potential energy due to the deformations of flexible substructures is equal to the sum of strain energy of flexible substructures and the potential energy due to the external forces acting on the substructures with minus sign. The total potential energy of flexible substructures can be found by summing each potential energy of all numbers of flexible elements,

$$E_{pa} = \frac{1}{2}\,\mathbf{d}^T\,\mathbf{K}\mathbf{d} - \mathbf{d}^T\,\mathbf{F}_a \tag{4.41}$$

The total potential energy of spacecraft

A total potential energy of the spacecraft is the summing of its undeformed body potential energy and flexible substructures potential energy. So, it can be written;

$$E_p = E_{pr} + E_{pa} = E_{p,r}\,(\mathbf{r}_{i,b}) + \frac{1}{2}\,\mathbf{d}^T\mathbf{K}\mathbf{d} - \mathbf{d}^T\mathbf{F}_a \tag{4.42}$$

General linear differential equations of motion of a flexible spacecraft

In deriving general linear differential equations of motion of flexible spacecraft, it will use the Lagrangian operator;

$$L = E_k - E_p \tag{4.43}$$

The lagrange's equation of motion can be expressed in the following form:

$$\frac{d}{dt}\left(\frac{\partial L}{\partial q}\right) - \frac{\partial L}{\partial \dot{q}} + \frac{\partial S}{\partial \dot{q}} = F \tag{4.44}$$

where **q** is a displacement vector, **q̇ is the velocity vector,** *F* is a general external forces vector, and *S* is a Rayleigh's dissipation. The Rayleigh's dissipation is defined as

$$S = \frac{1}{2}\dot{q}^T \mathbf{D}\, \dot{q} \tag{4.45}$$

where **D** is a system damping matrix.

The translational motion equation can be written as:

$$m\ddot{r} + \mathbf{Q}\,\dot{\omega} + \mathbf{W}\ddot{d} = \mathbf{F}_b \tag{4.46}$$

while rotational motion is:

$$\mathbf{Q}^T\ddot{r} + \mathbf{I}\dot{\omega} + \mathbf{A}\ddot{d} = \mathbf{T}_b \tag{4.47}$$

A linear expression for ω can be derived and written in the following form:

$$\omega = \dot{\theta} + \tilde{\omega}_o\, \theta + \omega_o \tag{4.48}$$

The above equations are nonlinear differential equations. If rigid body motions and flexible substructure deformations of the spacecraft are small, the higher order terms in the equations can be neglected. So, for small motions and displacements of a flexible spacecraft, the above equations can be simplified as:

$$m\ddot{r} + \mathbf{Q}\dot{\omega} + \mathbf{W}\ddot{d} = F_b \tag{4.49}$$

$$\mathbf{Q}^T\ddot{r} + \mathbf{I}\dot{\omega} + \mathbf{A}\ddot{d} = \mathbf{T}_b \tag{4.50}$$

$$\mathbf{M}\dot{d} + \mathbf{W}^T\dot{r} + \mathbf{A}^T\omega + \mathbf{D}\dot{d} + \mathbf{K}d = \mathbf{F}_b \tag{4.51}$$

27

By using the expression, the motion equations can also be written as

$$
\begin{bmatrix} m\mathbf{U}_3 & Q & W \\ Q^T & I & A \\ W^T & A^T & M \end{bmatrix} \begin{Bmatrix} \ddot{r} \\ \ddot{\theta} \\ \ddot{d} \end{Bmatrix} + \begin{bmatrix} \mathbf{0}_3 & Q\widetilde{\omega}_0 & \mathbf{0}_{3 \times nf} \\ \mathbf{0}_3 & I\widetilde{\omega}_0 & \mathbf{0}_{3 \times nf} \\ \mathbf{0}_{nf \times 3} & A^T\widetilde{\omega}_0 & D \end{bmatrix} \begin{Bmatrix} \dot{r} \\ \dot{\theta} \\ \dot{d} \end{Bmatrix} + \begin{bmatrix} \mathbf{0}_3 & \mathbf{0}_3 & \mathbf{0}_{3 \times nf} \\ \mathbf{0}_3 & \mathbf{0}_3 & \mathbf{0}_{3 \times nf} \\ \mathbf{0}_{nf \times 3} & \mathbf{0}_{nf \times 3} & K \end{bmatrix} \begin{Bmatrix} r \\ \theta \\ d \end{Bmatrix}
$$

$$
= \begin{Bmatrix} F_b \\ T_b \\ F_a \end{Bmatrix} \tag{4.52}
$$

where nf is the total number of degrees-of-freedom of the flexible substructures.

If the flexible substructures are supposed to have proportional damping properties, the damping matrix **D** can be formed by linear combination of system mass matrix **M** and stiffness matrix **K**;

$$
\mathbf{D} = \mu\,\mathbf{M} + \kappa\,\mathbf{K} \tag{4.53}
$$

Where for a certain flexible structure μ and κ are constants determined from two given damping ratios that correspond to two unequal natural frequencies of vibration.

4.2 A PARTICULAR MODEL OF A SATELLITE WITH TWO FLEXIBLE SOLAR PANELS

According to S. Parman's work, mathematical model for a hypothetical flexible satellite consisting of a rigid central body and two symmetrical solar panels have been developed [2]. The mass matrix and the stiffness matrix will be evaluated. The damping matrix of the solar panels will be assumed to be a proportional damping matrix. The solar arrays will be modeled as a number of rectangular plate elements by using the finite element method.

Model Idealization

According to reference [2], the data for the hypothetical satellite are chosen to a certain extent arbitrarily, as below:

1. The orbit is circular with $\omega_0 = 1$ rotation/day (or about 7.3×10^{-5} rad/sec). When there are no attitude errors, the Z-axis of main body fixed frame should point to

the centre of the earth, the Y-axis is normal to the orbit plane, and the X-axis completes the orthogonal set by following the right-hand-side law, that is, should point to the velocity of the satellite.

2. Two large solar panels are attached with the longitudinal axis in the Y-axis direction of the main body fixed reference frame, and oriented toward the sun. So, the inertia matrix $\mathbf{I_a}$ of flexible solar panels should vary with time for an orbital period. However, for the relatively short time intervals considered, this matrix will be assumed to be constant.

3. The translational displacements of the rigid main body are not assumed to be zero. It means that the origin of inertial reference frame does not always coincide with the origin of main body fixed frame. The origin of main body fixed reference frame is chosen at the middle of longitudinal axis of the solar panels. In this case, the Y-axis of the main body fixed frame coincides with the longitudinal axis of the solar panels. The origin of main body fixed reference frame not always coincides with the mass centre of the whole satellite.

The configuration of the satellite is shown in Figure 5.
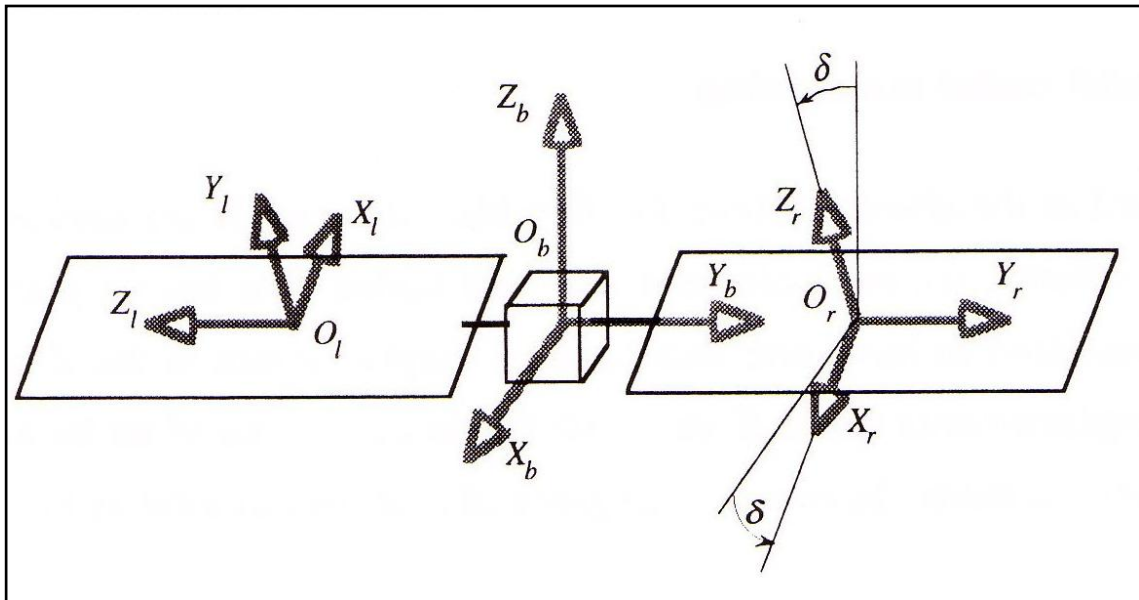
Figure 8 The configuration of flexible satellite for simulation

The solar panels are flat plate structures; the transformation matrix for each panel will be the same for any plate element. For the application of the finite element method, the following choices are considered:

1. The solar panels are divided into rectangular flat plate bending elements.
2. Each element has a uniform mass density ρ_i.
3. Only out-of-plane deformations of the solar panels are considered.
4. External forces and torques on the solar panels are assumed to work on the nodal points of the elements. The rigid central body is allowed to rotate due to the external torques and to translate due to the external forces.
5. The Y-axis of main body fixed frame and the Y-axis of the solar panel local reference frames are parallel or ant parallel. The X and Y-axis of local reference frames are in the panel plane, and their Z-axis are normal to the plane.

By using 2nd simplification according to figure 5, the transformation matrices form the main body fixed frame to the flexible solar panel local reference frames are reduced to two pieces for the solar panels. For the right hand side solar panel, the transformation matrix is;

$$\mathbf{T}_l = \begin{bmatrix} -\cos\delta & 0 & -\sin\delta \\ 0 & -1 & 0 \\ \sin\delta & 0 & \cos\delta \end{bmatrix} \tag{4.54}$$

and for the left hand side solar panel, the transformation matrix is:

$$\mathbf{T}_r = \begin{bmatrix} -\cos\delta & 0 & -\sin\delta \\ 0 & -1 & 0 \\ \sin\delta & 0 & \cos\delta \end{bmatrix} \tag{4.55}$$

where δ is the offset angle of the flexible solar panels.

4.2 ATTITUDE MANEUVERS OF A SATELLITE WITH FLEXIBLE SOLAR PANELS UNDER BANG-BANG COMMANDS

Most of the telecommunication devices are placed in the rigid main body. The movement of the satellite is represented by the linear and rotational motion of the main body. To determine the inputs for the satellite to move its orientation the satellite will be considered as a rigid body. With respect to the center of mass of the satellite in the undeformed state, the acceleration of the center of mass under control or external forces worked on it can be expressed as [1];

$$\ddot{\vec{r}} = \frac{1}{m}\ \vec{F_b} \tag{4.56}$$

$$\ddot{\vec{\Theta}} = I^{-1}\ \vec{T_b} \tag{4.57}$$

where $\ddot{\vec{r}}$ and $\ddot{\vec{\Theta}}$ are translational and rotational acceleration vectors of the rigid main body, $\vec{F_b}$ and $\vec{T_b}$ are external force and torque vectors working on the main body of satellite, m is the total mass of satellite, and $\mathbf{I}$ is the total inertia matrix of satellite.

The desired velocity of satellite as an undeformed body can be calculated by integrating equation 4.56 and 4.57 with respect to time, the desired displacements of satellite as undeformed state can be found,

$$\dot{\mathbf{r}}_d = \int \frac{1}{m} \mathbf{F_b}\ dt \tag{4.58}$$

and

$$\dot{\mathbf{\Theta}}_d = \int I^{-1} \mathbf{T_b}\ dt \tag{4.59}$$

where $\dot{\mathbf{r}}_d$ and $\dot{\mathbf{\Theta}}_d$ are the desired translational and rotational velocities of the main body. Integrations once again of equation 4.4 and 4.5 with respect to time, the desires displacements of satellite as undeformed state can be found,

$$\mathbf{r}_d = \iint \frac{1}{m} \mathbf{F_b}\ dt\ dt \tag{4.60}$$

31

and

$$\mathbf{\Theta}_d = \iint I^{-1} \, \mathbf{T}_b \, dt \, dt \tag{4.61}$$

where $\mathbf{r}_d$ and $\mathbf{\Theta}_d$ are the desired translational and rotational displacements of the undeformed satellite.

Slew maneuvers of spacecraft in operation can be classified into two categories: *spinning up to constant velocity slew maneuvers and rest-to-rest slew maneuver.* In a spinning up to constant velocity slew maneuver, the spacecraft has certain or zero velocity in the initial, then it is given an input to increase or decrease its velocity to the desired constant value at the end of maneuver, i.e

$$\dot{\mathbf{r}}_d = \text{constant} \tag{4.62}$$

for the translational slew maneuver, and

$$\dot{\mathbf{\Theta}}_d = \text{constant} \tag{4.63}$$

for the rotational slew maneuver. In a rest-to-rest slew maneuver, the spacecraft has no initial velocity, then it is given an input to move or maneuver the spacecraft to the desired displacement with the final velocity equals to zero. It means that

$$\dot{\mathbf{r}}_d = \mathbf{0}, \, \mathbf{r}_d = \text{constant} \tag{4.64}$$

for the translational slew maneuver, and

$$\dot{\mathbf{\Theta}}_d = 0, \, \mathbf{\Theta}_d = \text{constant} \tag{4.65}$$

for rotational slew maneuver.

For the spacecraft maneuvering under constant magnitude force or torque inputs, a single input gives the spinning up to constant velocity slew maneuver in optimal time, while the rest-to-rest slew maneuver with optimal time will be resulted by a bang-bang input. In this paper, the spinning-up to constant velocity slew maneuvers will not be discussed. Only the rest-to-rest attitude maneuvers of the flexible satellite will be studied.

To simulate the dynamics of the satellite, the parameters of flexible solar panels are listed in the table 1 and the parameters of the rigid main body chosen are listed in table 2. The con figuration of the satellite used in simulations is shown in figure

Table 1: Parameters of flexible solar panels of satellite

Description	Values
Number of solar panels	2
Dimension of each solar panel (m)	12 x 2.4 x 0.3
Young Modulus, E (N/m²)	0.6×10^8
Poisson ratio ν	0.3
Mass density, ρ (kg/m³)	120
Number of elements in each solar panels	16
Dimension of each element b x a x a t(m)	1.5 x 1.2 x 0.03
Number of nodes in each element	4
Number of nodes in each solar panel	27
Number of degrees of freedom of each node	3 (1 translation and 2 rotations)
Total degrees of freedom of solar panels	144, i.e 2 x 3 x (27-3)
Offset angle, δ (degrees)	30
Damping coefficients, (μ,κ)	(0,0)
Distance between panel's root and O_b (m)	1.80

Table 2 : Masses of the rigid body of satellite and their positions with respect to the origin of rigid main body reference frame O_b

Rigid body lumped mass (kg)	Position (m) (x_b, y_b, z_b)
400	(0.40, 0.00, 0.00)
400	(-0.40, 0.00, 0.00)
500	(0.00, 0.50, 0.00)
500	(0.00, -0.50, 0.00)
550	(0.00, 0.00, 1.40)
550	(0.00, 0.00, -1.40)

For the rigid main body of satellite, it consisted of 6 lumped masses at certain positions relative to the origin of the main body-fixed reference frame as shown in the table 2. The offset angles of solar panels δ are 0 degrees. The damping properties for these solar panels are neglected (μ, κ). The orbital frame moves relative to the inertial frame with constant angular velocity

$$\boldsymbol{\omega_o} = \omega_o \boldsymbol{j}_i \tag{4.66}$$

where $\boldsymbol{j}_i$ is the unit vector in Y_i-axis direction, $\omega_o = 7.29\ 10^{-5}$ rad/sec, so that F_o performs in F_i one rotation per sidereal day (24 hours of sidereal time or 23.93446 hours).
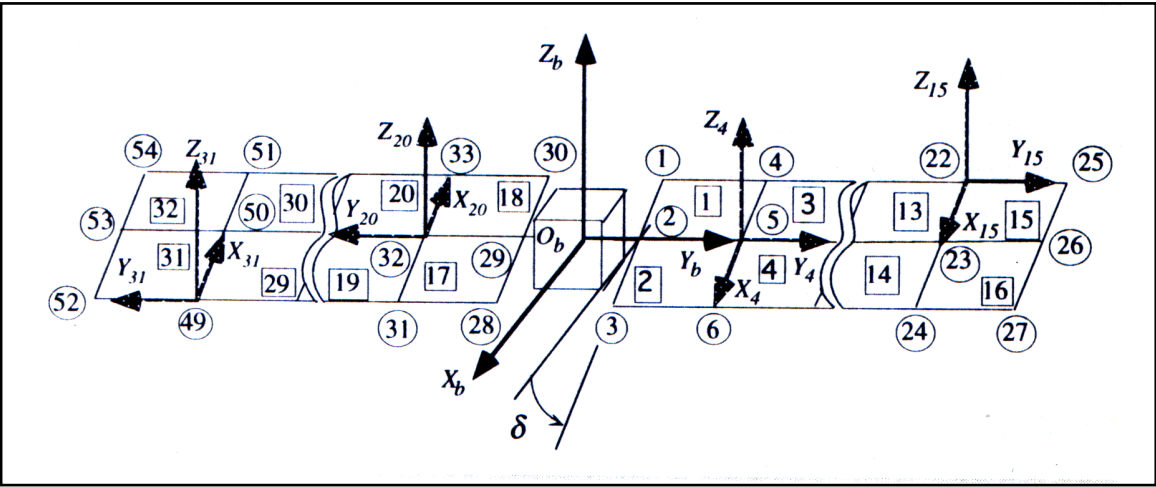
Figure 9 The satellite model used in the simulations

Simulation 1: Attitude Maneuvers of the Flexible Satellite under Bang-Bang Torque Inputs with initial angle Φ_i = -4°, θ_i = 5°, ψ_i = -3° - angle displacement

The initial attitude displacements in this simulation are **-4°** in roll, **5°** in pitch, and **-3** in yaw angle. The desired attitude displacements in this simulation are 0° in all angles. The amplitude of commands for T_{bx}, T_{by}, and T_{bz} is 2N-m. The satellite is subjected to the roll torque command, the pitch torque command, and the yaw torque command simultaneously. With these inputs, the attitude angles move to the desired values. The amplitude of the residual roll angle oscillations is about 0.89°, while the amplitude of the yaw oscillation is 0.47° as shown in figure 9. Such residual oscillations are unfavorable and may disturb the satellite mission. The residual pitch angle oscillation of the satellite studied here is smaller compared to others; 0.03°.
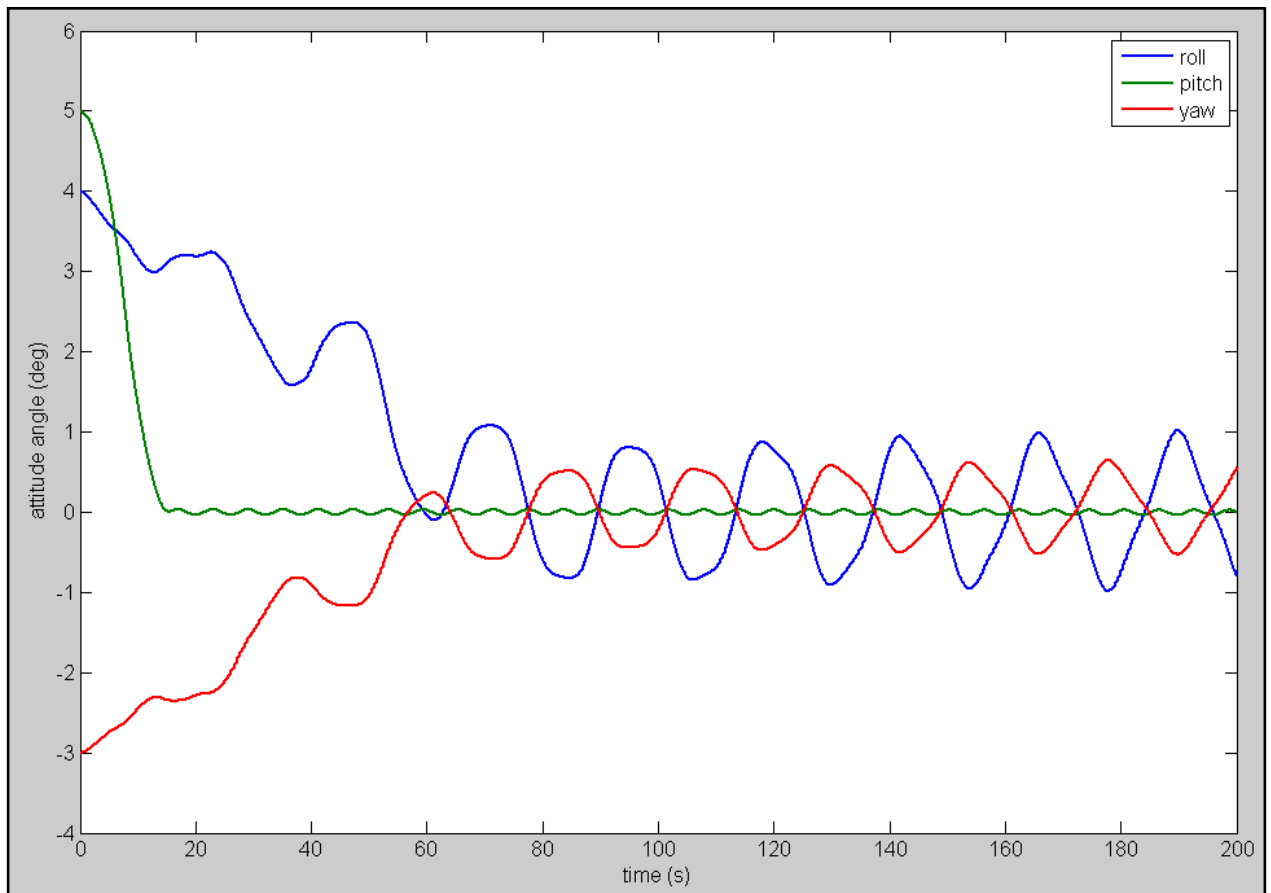
Figure 10 Time response of attitude angles for Φ_i = -4°, θ_i = 5°, ψ_i = -3°

The response time for each angle displacement are presented in the figure below:

Time response for roll angle, Φ;
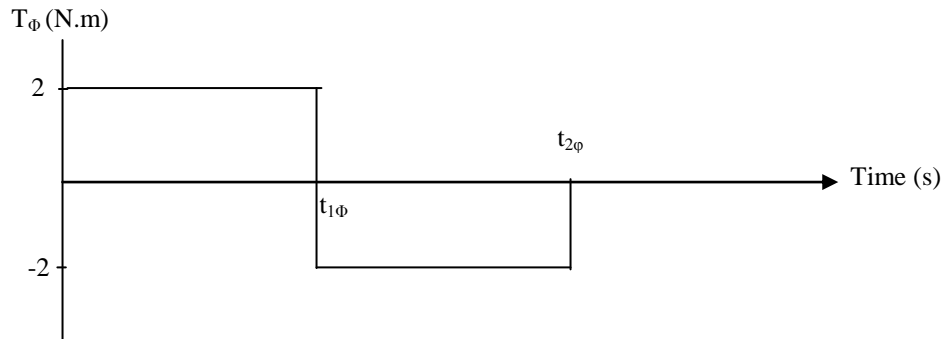
$t_{1\Phi} = 38.82s$
$t_{2\Phi} = 77.64s$

Time response for pitch angle, θ;
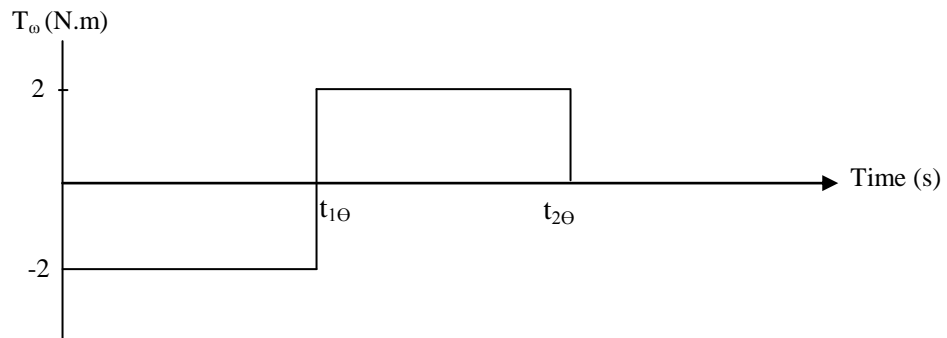
$t_{1\theta} = 9.14 \text{ s}$
$t_{2\theta} = 18.28s$

Time response for yaw angle, ψ;
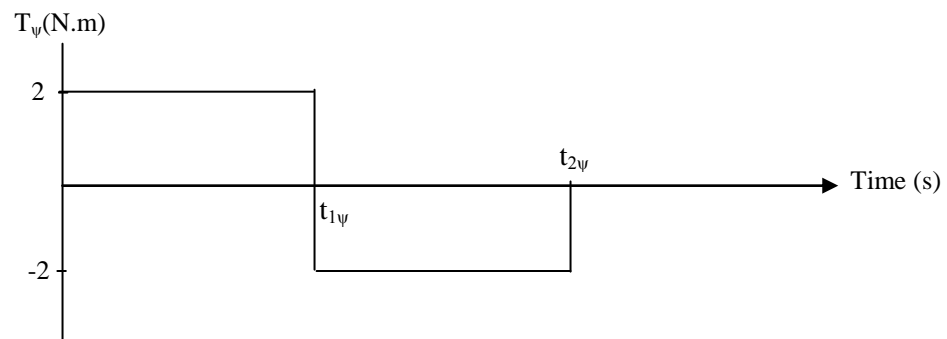
$t_{1\psi} = 38.77s$
$t_{2\psi} = 77.54s$

4.4 ATTITUDE MANEUVERS OF A SATELLITE WITH FLEXIBLE SOLAR PANELS UNDER PD CONTROLLER

The same equations of motion of flexible spacecraft that was used in the bang-bang control commands will be used in PD controller. The torque commands have been change according to the time-optimal control behavior. In liner range the torque command T_c will have the following expression:

$$T_c = Ke + K_d\dot{e} \qquad (4.65)$$

where K and K_d are computed in standard way for a second-order linear feed-back system.

Equation 4.65 can also be written in the form;

$$\begin{Bmatrix} \mathbf{T}_{cx} \\ \mathbf{T}_{cy} \\ \mathbf{T}_{cz} \end{Bmatrix} = \begin{bmatrix} K_\phi & 0 & 0 \\ 0 & K_\theta & 0 \\ 0 & 0 & K_\psi \end{bmatrix} \begin{Bmatrix} e_\phi \\ e_\theta \\ e_\psi \end{Bmatrix} + \begin{bmatrix} K_{d\phi} & 0 & 0 \\ 0 & K_{d\theta} & 0 \\ 0 & 0 & K_{d\psi} \end{bmatrix} \begin{Bmatrix} \dot{e}_\phi \\ \dot{e}_\theta \\ \dot{e}_\psi \end{Bmatrix} \qquad (4.66)$$

If K_ϕ, K_θ, and K_ψ are selected in the same values, equation 4.66 can also be written in this form;

$$\begin{Bmatrix} \mathbf{T}_{cx} \\ \mathbf{T}_{cy} \\ \mathbf{T}_{cz} \end{Bmatrix} = \mathrm{K} \begin{Bmatrix} e_\phi \\ e_\theta \\ e_\psi \end{Bmatrix} + \mathrm{K}_d \begin{Bmatrix} \dot{e}_\phi \\ \dot{e}_\theta \\ \dot{e}_\psi \end{Bmatrix} \qquad (4.68)$$

If the closed-loop feedback system is to have a natural frequency ω_n and a damping coefficient ξ, then

$$K = \omega_n I \quad \text{and} \quad K_d = 2\,\xi\omega_n I \qquad (4.67)$$

But, in this work, K and K_d are determined by using trial and error to find the suitable damping response of the satellite. Then, by choosing suitable response, the value K and K_d will be kept constant in the next simulation using thruster logic. The general closed-loop structure of PD control shown in figure 10, 11 and 12 for each angle;
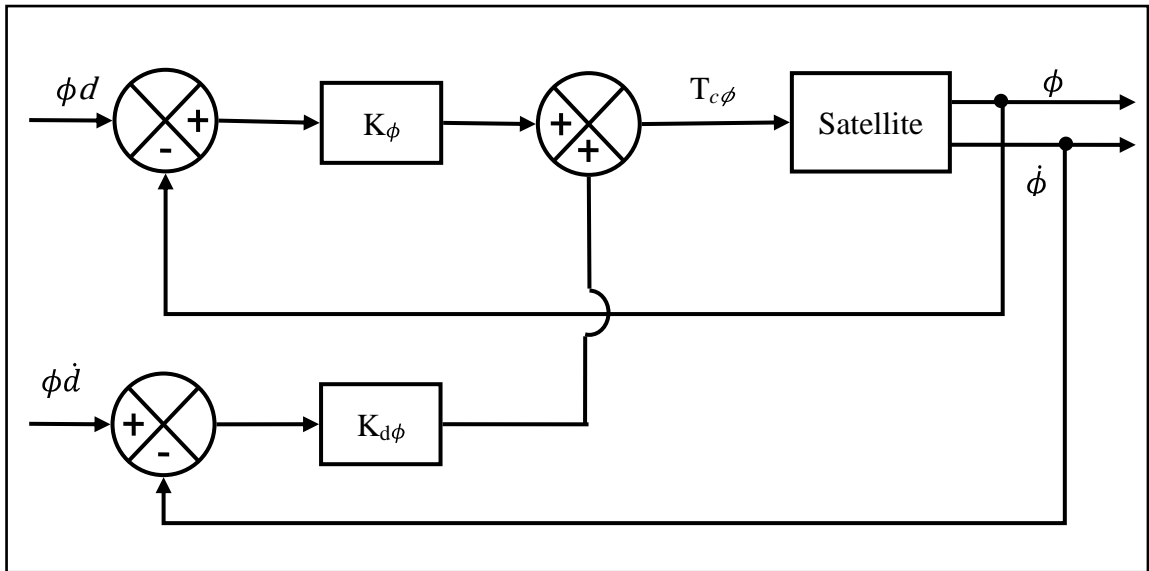
Figure 11 Block diagram of a closed-loop PD controller for ϕ angle
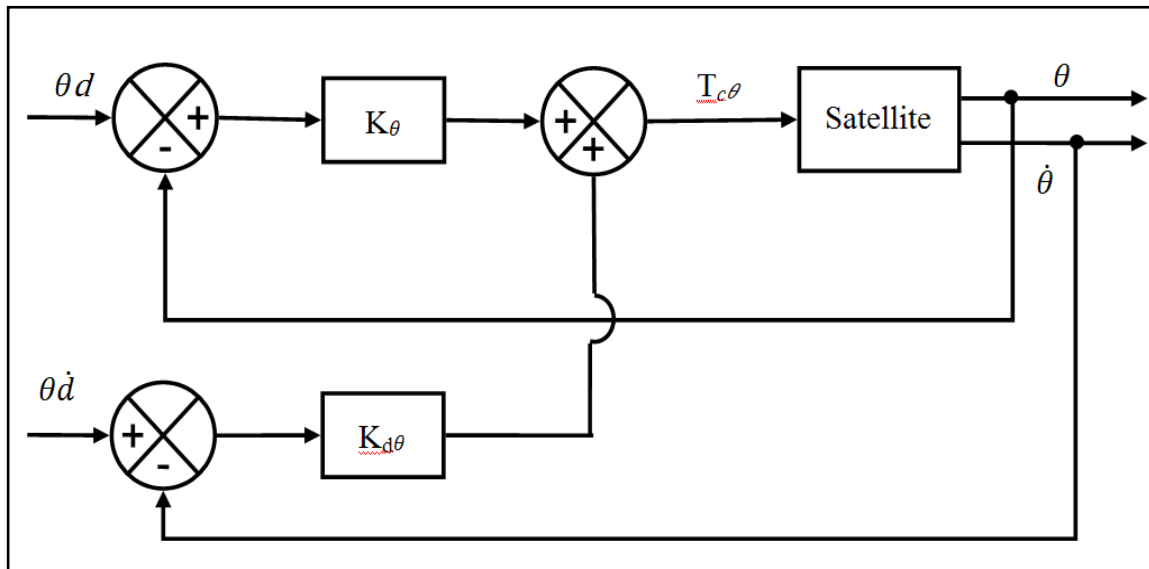
Figure 12 Block diagram of a closed-loop PD controller for $\boldsymbol{\theta}$ angle
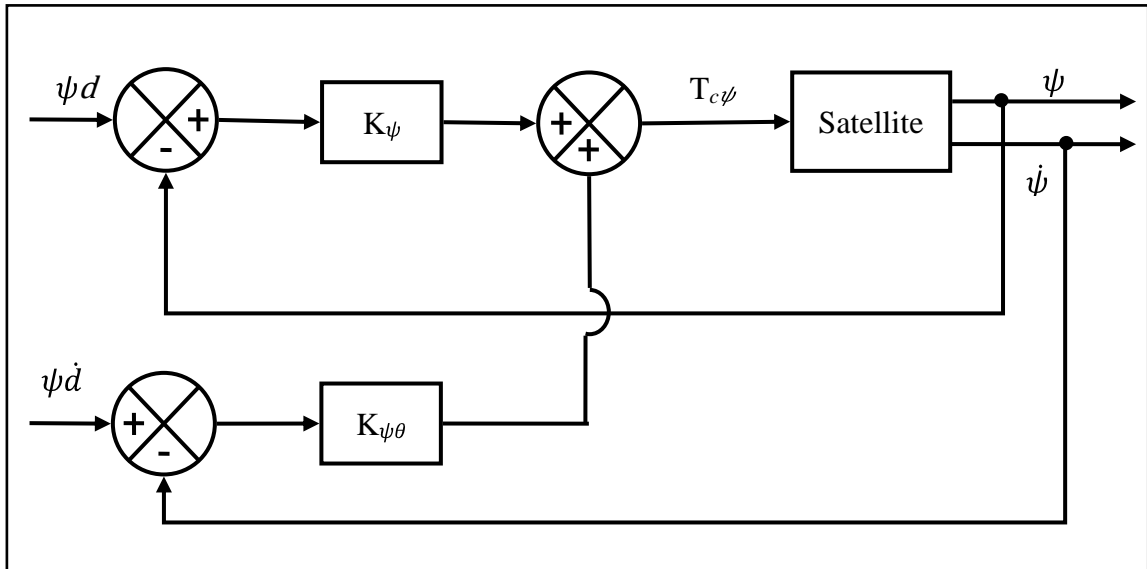
Figure 13 Block diagram of a closed-loop PD controller for ψ angle

For the simulation that has been done, the K and K_d was varied to achieve a stabile response. By varying the K and K_d, the response also varied. The simulation is done based on below pattern:

Table 3 Variation of stifnees costant used in simulations

K\K$_d$	1	10	100	1000
1	Sa1	Sa2	Sa3	Sa4
10	Sb1	Sb2	Sb3	Sb4
100	Sc1	Sc2	Sc3	Sc4
1000	Sd1	Sd2	Sd3	Sd4

The simulations are numbered as in above table 3. The next simulations *a1, a3, b4* and *c4* below, are some examples of the result using different constant. In the variation of stiffness constant, table 3, the results sometimes have large oscillation. From the simulations, only five were picked to have the nearest to the desired oscillation. Then, simulations were done again with the same controller but with smaller variation of stiffness constant.

During the simulation, the time for the cycle needs to vary from one simulation to another. This is because the response time differs when K and K_d change. All of the simulations have constant initial attitude displacements (roll: **4°**, pitch: **5°**, and yaw: **-3°**) and desired attitude displacement which is 0°.

Example 1 – using PD controller

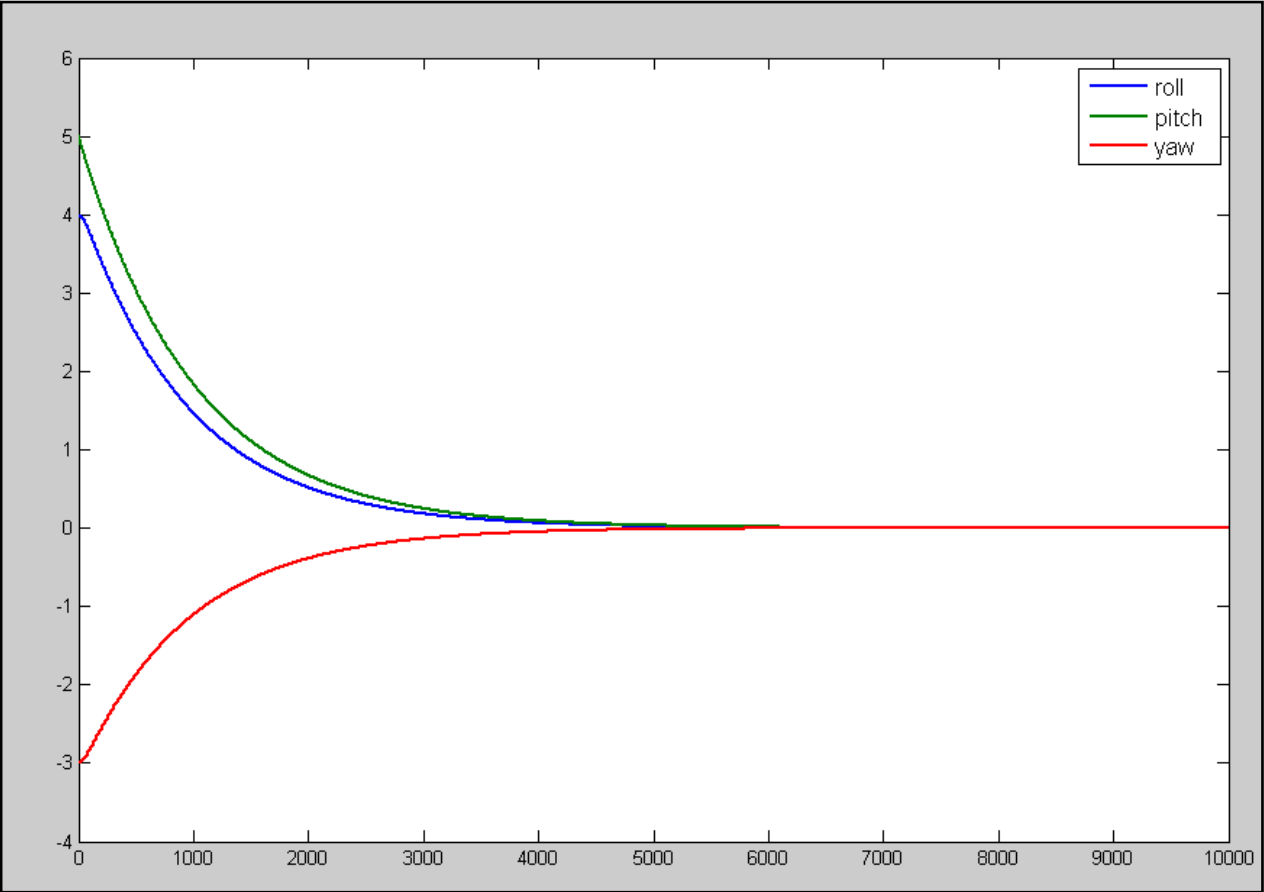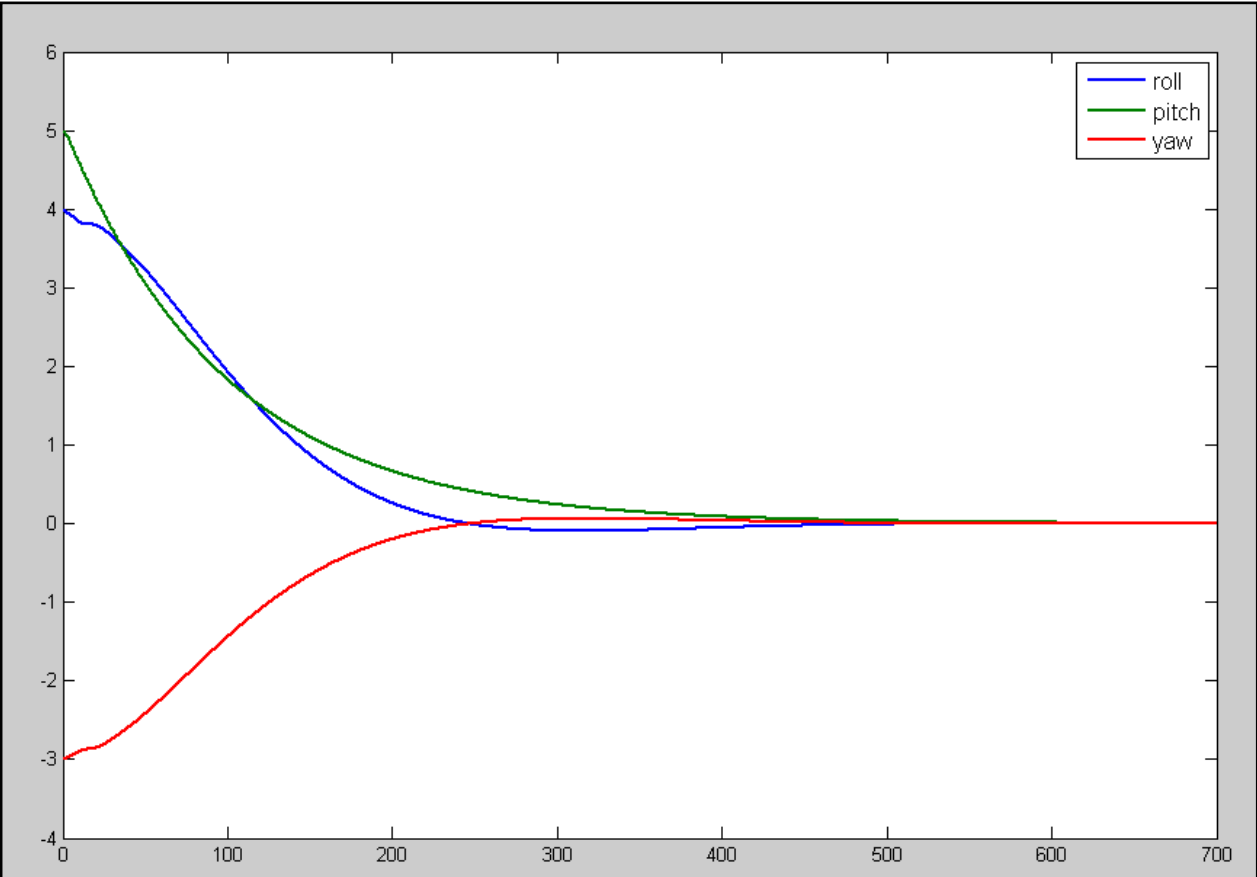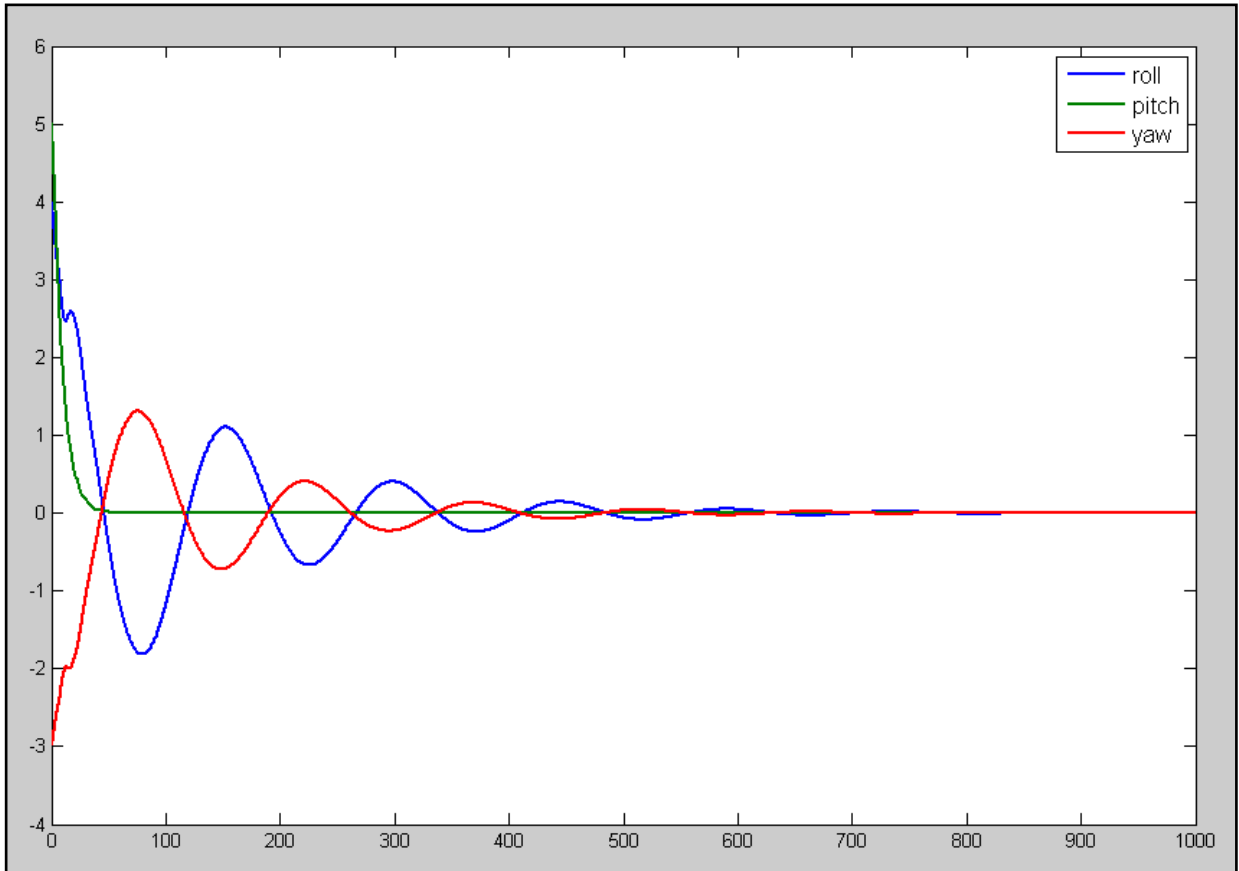*Simulation a1: Attitude Maneuvers of the Flexible Satellite* **(K= 1, Kd= 1, t=2000)**
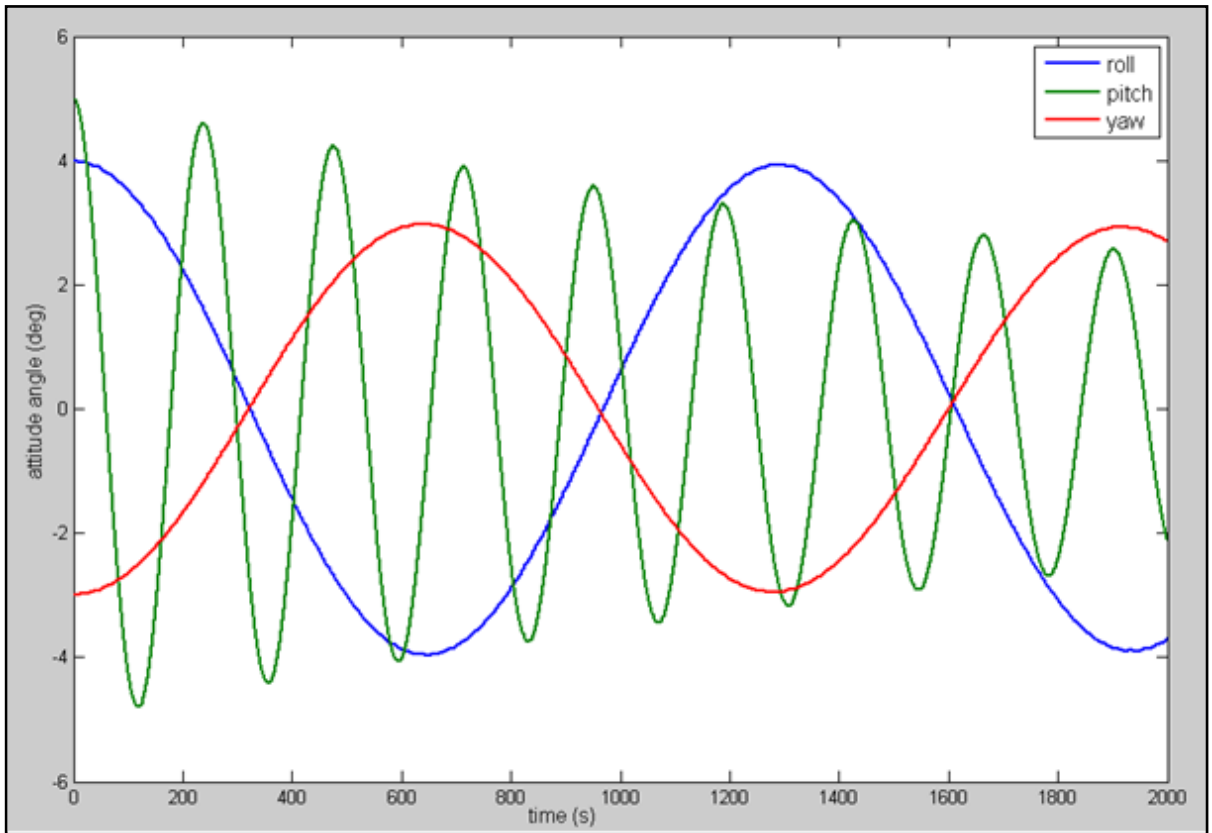
Figure 14 Attitude Maneuvers of the Flexible Satellite **(K= 1, Kd= 1, t=2000)**

The stiffness of the panels are set to be, K=1 and K_d=1. Roll, pitch, and yaw torques will all be needed to change the roll, pitch, and yaw angles to the desired values. The satellite is subjected firstly to the roll torque command, then the pitch torque command, and lastly the yaw torque command. With these inputs, the attitude angles move to the desired values.

40

After the maneuvers, the roll angles oscillate in large amplitudes at the period of **1286.8** seconds, while the yaw angles oscillate in slightly smaller amplitudes at the period of **1279.4** seconds. The amplitude of the pitch angle is **233.4** seconds. The amplitude of the residual roll angle oscillations is about **3.95°,** while the average amplitude of the pitch oscillation is **3.52°,** and the smallest angle studied here is the yaw angle**,** with **2.96°.** Such residual oscillations are unfavorable and may disturb the satellite missions.

Example 2 – using PD controller

Simulation a3: Attitude Maneuvers of the Flexible Satellite **(K= 1, Kd= 100, t=5000)**
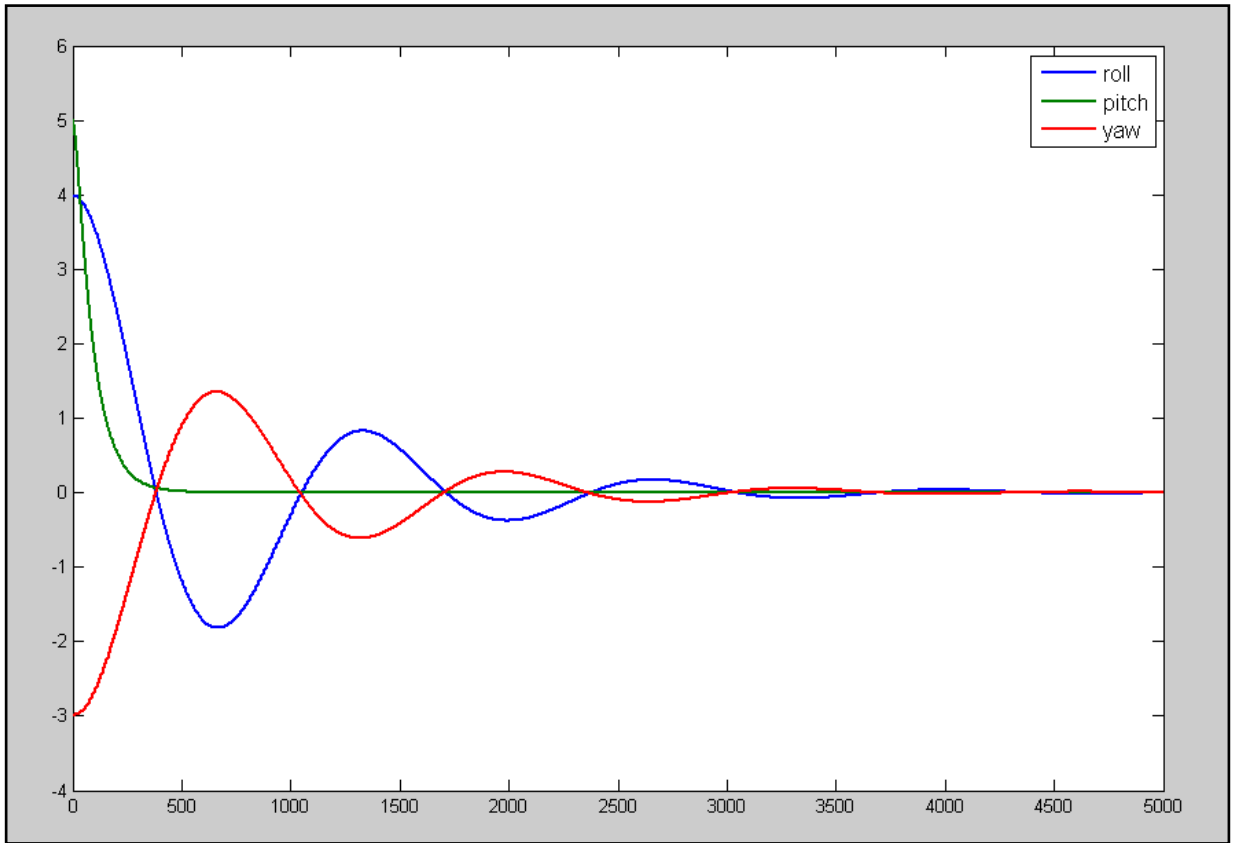
Figure 15 Attitude Maneuvers of the Flexible Satellite **(K= 1, Kd= 100, t=5000)**

The stiffness of the panels are set to be, K=1 and K_d=100. After the maneuvers, the roll angles oscillate in large amplitudes at the period of **4329** seconds, while the yaw angles oscillate in slightly smaller amplitudes at the period of **4318.6** seconds. The amplitude of the residual roll angle oscillations is about **0.02°,** while the average amplitude of the yaw

oscillation is **0.01°.** The residual pitch angle oscillation of the satellite studied here is very small**.**

Example 3 – using PD controller

Simulation a4: Attitude Maneuvers of the Flexible Satellite **(K= 1, Kd= 1000, t=10000)**

Figure 16 Attitude Maneuvers of the Flexible Satellite **(K= 1, Kd= 1000, t=10000)**

The stiffness of the panels are set to be, K=1 and K_d=1000. After the maneuvers, the roll, yaw and pitch angles oscillation is very small.

42

<u>Example 4 – using PD controller</u>

Simulation b4: Attitude Maneuvers of the Flexible Satellite **(K= 10, Kd=1000, t=700)**

Figure 17 Attitude Maneuvers of the Flexible Satellite **(K= 10, Kd=1000, t=700)**

The stiffness of the panels are set to be, K=10 and K_d=1000. After the maneuvers, the roll, yaw and pitch angles oscillation is very small.

Example 5 – using PD controller

Simulation c4: Attitude Maneuvers of the Flexible Satellite **(K= 100, Kd=1000, t=1000)**

Figure 18 Attitude Maneuvers of the Flexible Satellite **(K= 100, Kd=1000, t=1000)**

The stiffness of the panels are set to be, K=100 and K_d=1000. After the maneuvers, the roll angles oscillate in large amplitudes at the period of **146.7** seconds, while the yaw angles oscillate in slightly smaller amplitudes at the period of **145.9** seconds. The amplitude of the residual roll angle oscillations is about **0.001°,** while the average amplitude of the yaw oscillation is **0.005°.** The residual pitch angle oscillation of the satellite studied here is very small**.**

Based on results of simulations, values of K and K_d in simulation 3 and 4 are selected for the next application of thruster control. For this case, the satellite can be menuevered in the shortest time without a lot of oscillation to achieve the new desired attitude, which is 0° in attitude angle. Simulation 2 is for the result of angle displacement of damping

44

response of the satellite. Simulation 3 is for the result of amplitude of torque for the initial command to the thruster.

Simulation 2: Attitude Maneuvers of the Flexible Satellite under PD controller with (**K= 100, Kd=2000, t=400**) – *angle displacement*
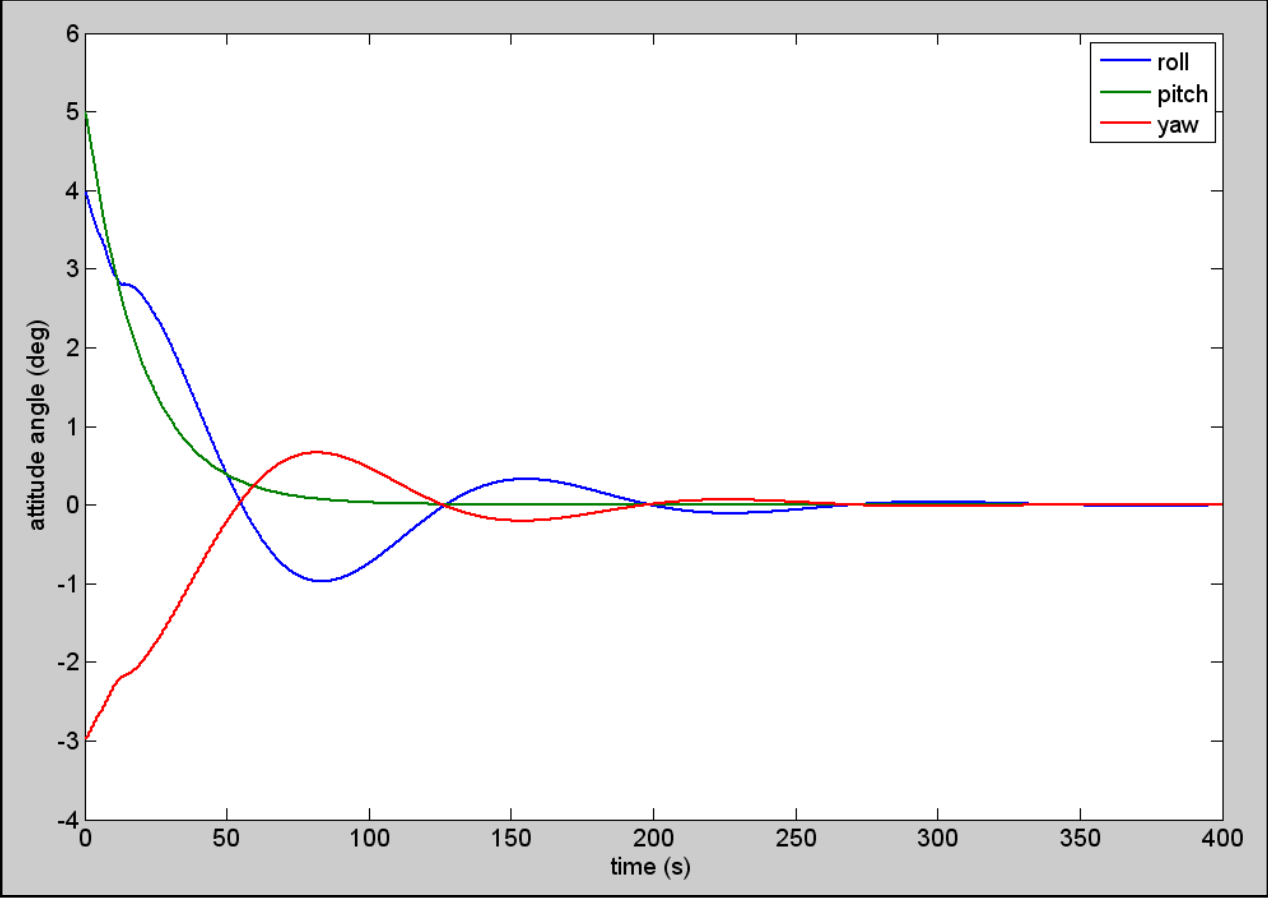
Figure 19 Attitude Maneuvers of the Flexible Satellite under PD control (**K= 100, Kd=2000, t=400**) – angle displacement

This is the chosen constant stiffness with the same parameters used in bang-bang controller. The initial attitude displacements in this simulation are **-4°** in roll, **5°** in pitch, and **-3** in yaw angle. The desired attitude displacements in this simulation are 0° in all angles. The satellite is subjected to the roll torque command, the pitch torque command, and the yaw torque command simultaneously. With these inputs, the attitude angles move to the desired values. The amplitude of the residual roll angle oscillations is about

0.0035°, while the amplitude of the yaw oscillation is 0.005° as shown in figure 19. Such residual oscillations are acceptable and the satellite mission will hope to run smoothly. The residual pitch angle oscillation of the satellite studied here is very small, nearly reach 0°.

Simulation 3: Attitude Maneuvers of the Flexible Satellite under PD controller with **(K= 100, Kd=2000, t=400)** *– amplitude torque*
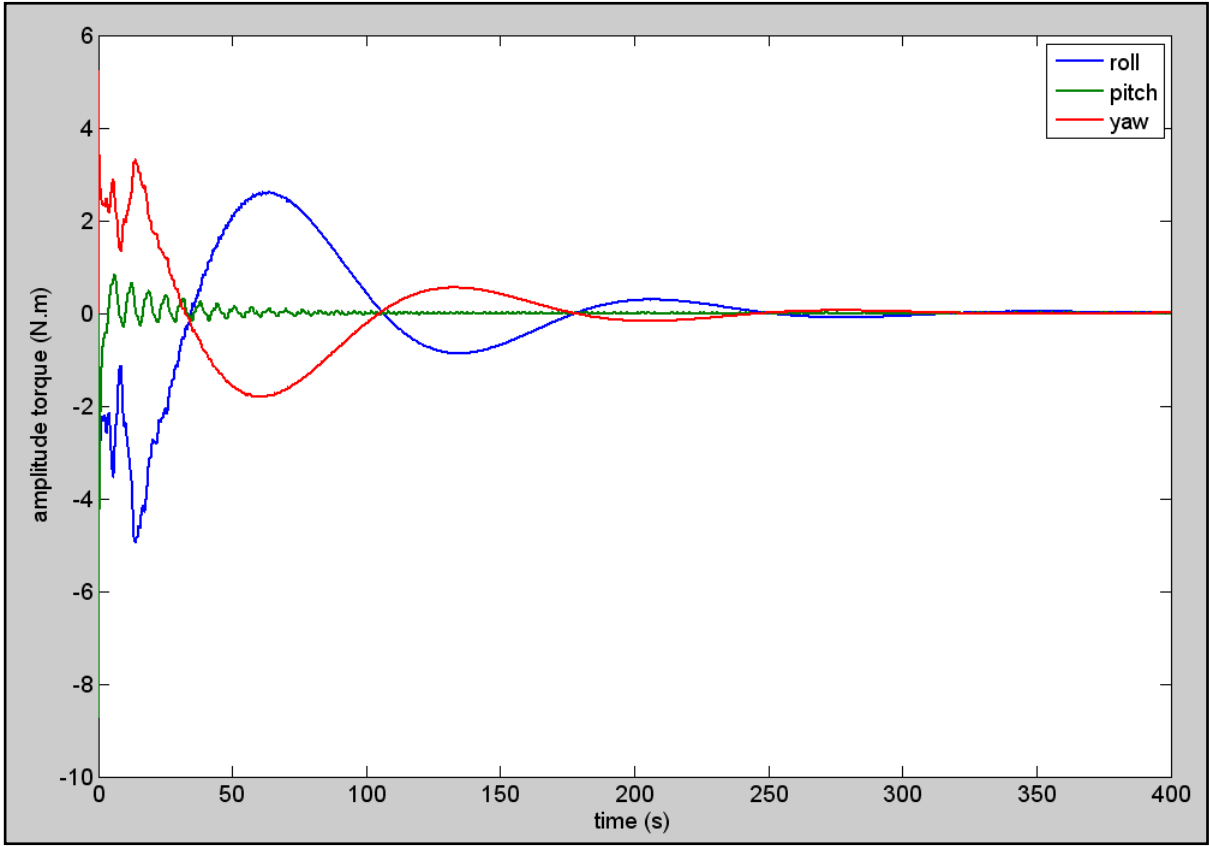
Figure 20 Attitude Maneuvers of the Flexible Satellite under PD control **(K= 100, K$_d$=2000, t=400)** – amplitude torque

Above is the simulation result for the amplitude of torque using PD controller.

4.5 ATTITUDE MANEUVERS OF A SATELLITE WITH FLEXIBLE SOLAR PANELS USING THRUSTERS BASED ON PD CONTROLLER LOGIC

Using the command for the PD controller, the command law will be adjusted to form the thruster output. Below are block diagram for the thruster based on PD controller logic;
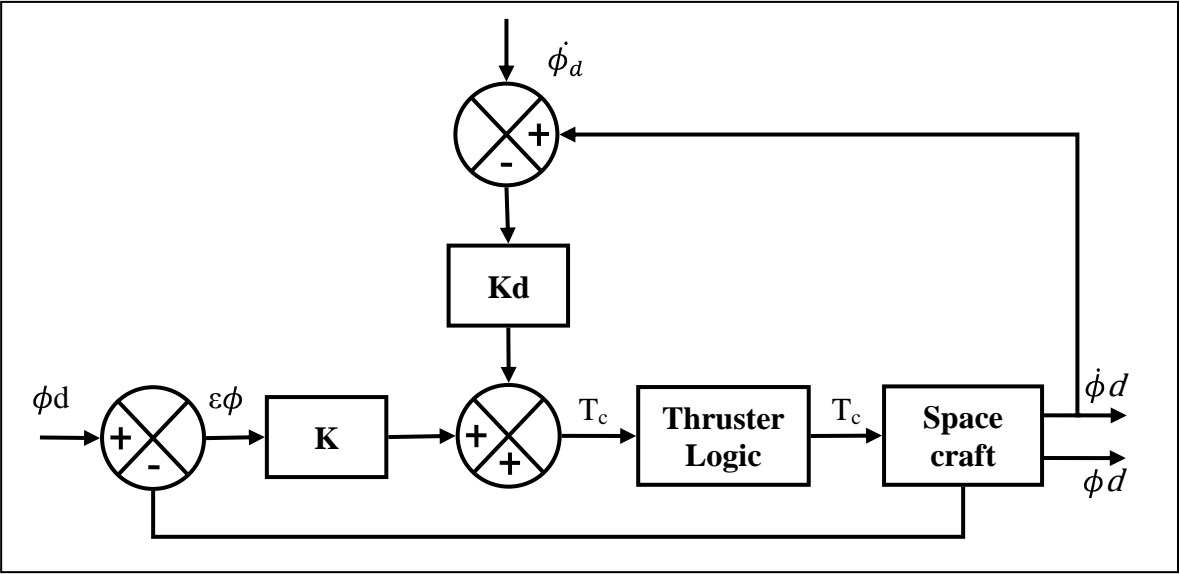
Figure 21 Block diagram of a closed-loop thruster based PD controller logic for ϕ angle
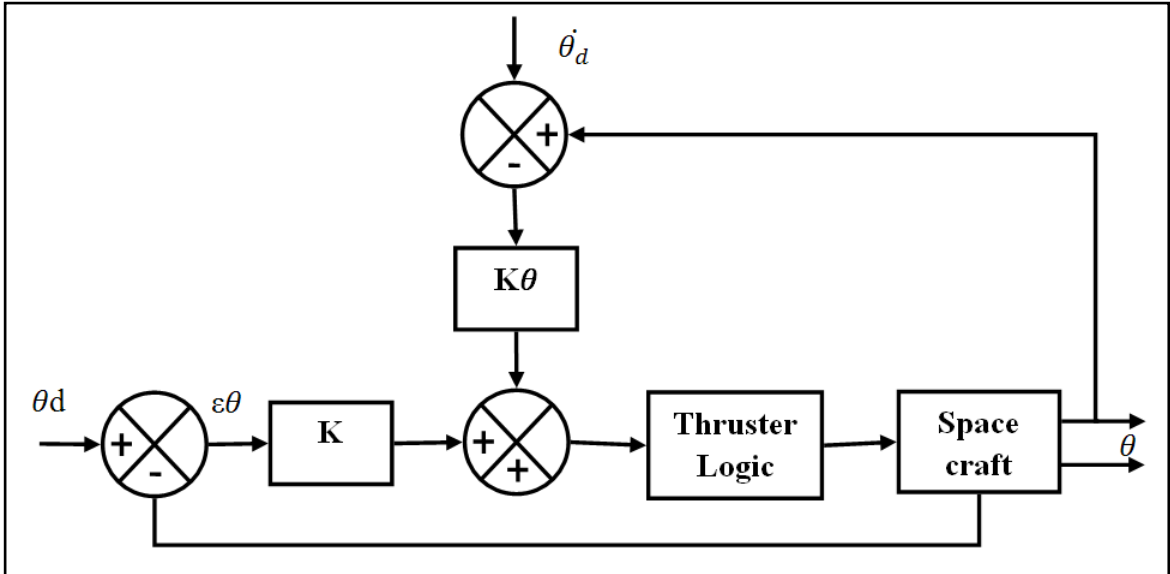
Figure 22 Block diagram of a closed-loop thruster based PD controller logic for θ angle
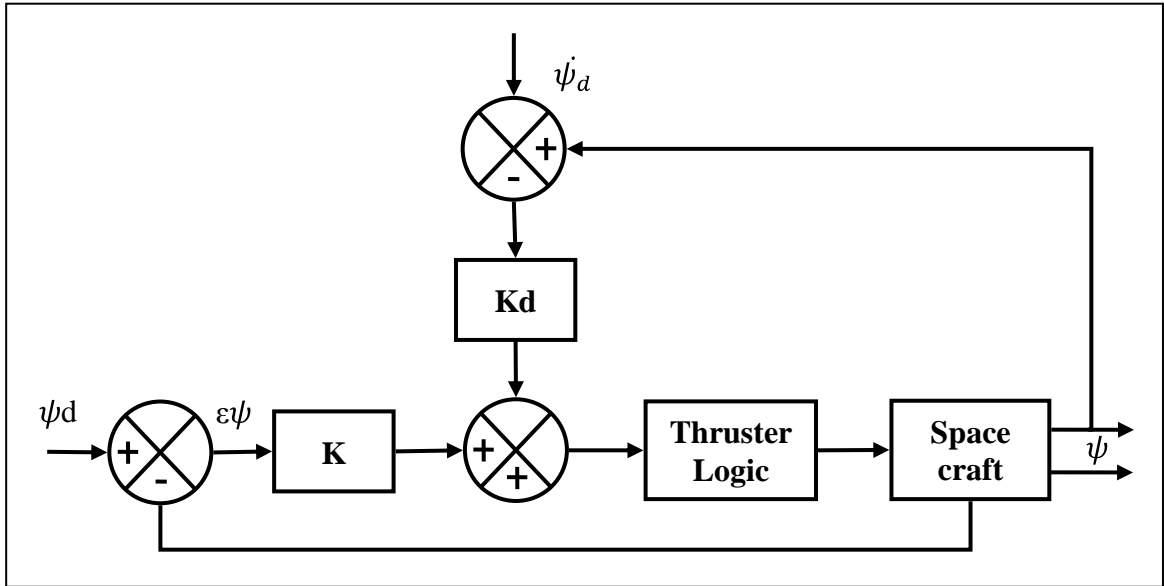
Figure 23 Block diagram of a closed-loop thruster based PD controller logic for ψ angle

The logic to implement thrusters can be seen in figure 24. T_c is the torque resulted by using PD controller. It must be applied for the torques in roll, pitch and yaw motions. $T_{c\,min}$ is the sensitivity value of torque given for the thruster application.
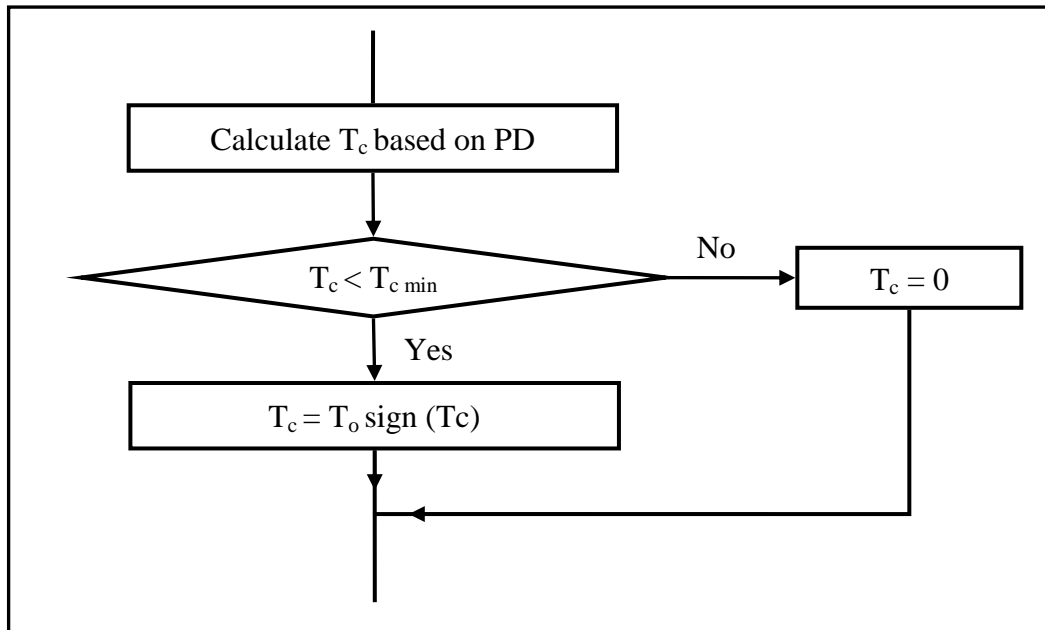
Figure 24 Logic to implement thrusters

Simulation 4: Attitude Maneuvers of the Flexible Satellite using thrusters based on PD controller with - angle displacement
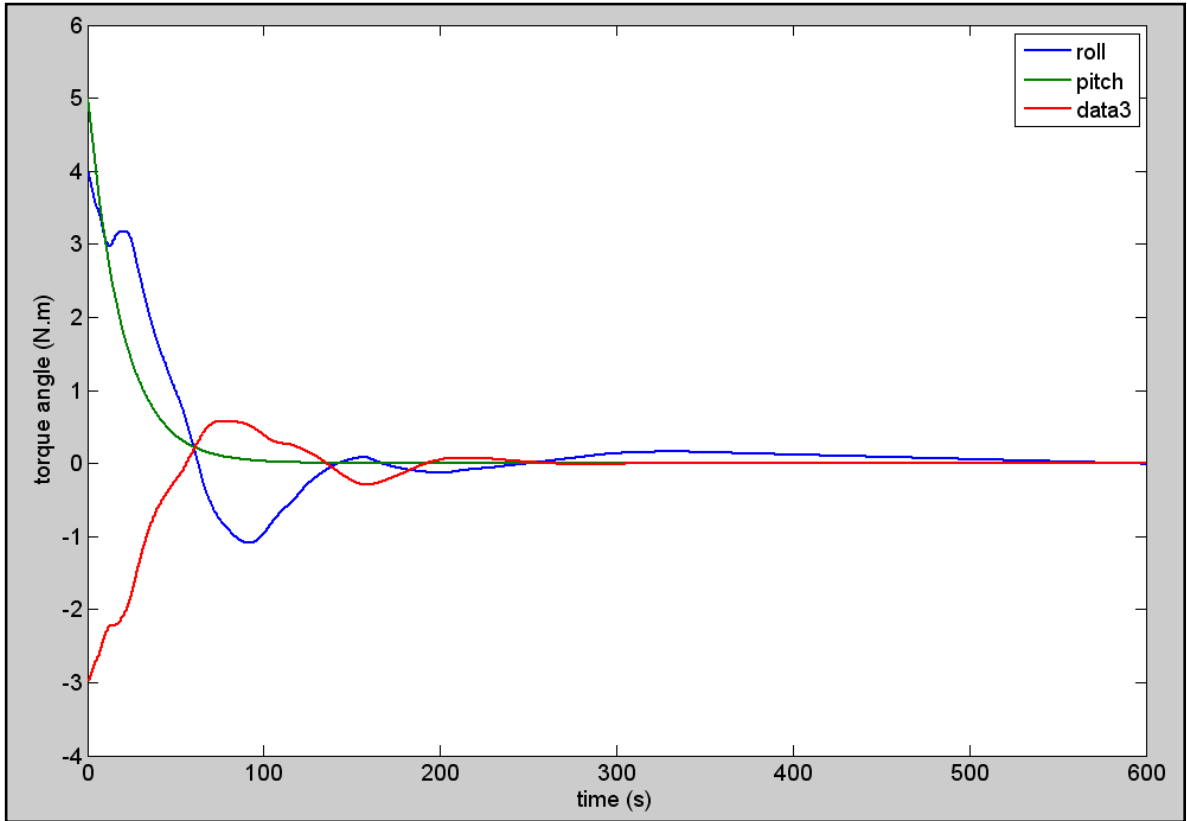
Figure 25 Attitude Maneuvers of the Flexible Satellite using thruster based on PD controller (K= 100, Kd=2000) – angle displacement

This is the chosen constant stiffness with the same parameters used in bang-bang controller. The initial attitude displacements in this simulation are **-4°** in roll, **5°** in pitch, and -**3** in yaw angle. The desired attitude displacements in this simulation are 0° in all angles. The satellite is subjected to the roll torque command, the pitch torque command, and the yaw torque command simultaneously. With these inputs, the attitude angles move to the desired values. The amplitude of the residual roll angle oscillations is about 0.0035°, while the amplitude of the yaw oscillation is 0.005° as shown in figure 25. Such residual oscillations are acceptable and the satellite mission will hope to run smoothly. The residual pitch angle oscillation of the satellite studied here is very small, nearly reach 0°.

Simulation 5: Attitude Maneuvers of the Flexible Satellite using thrusters based on PD controller with **(K= 100, Kd=2000, t=400)** *– amplitude torque of roll angle*
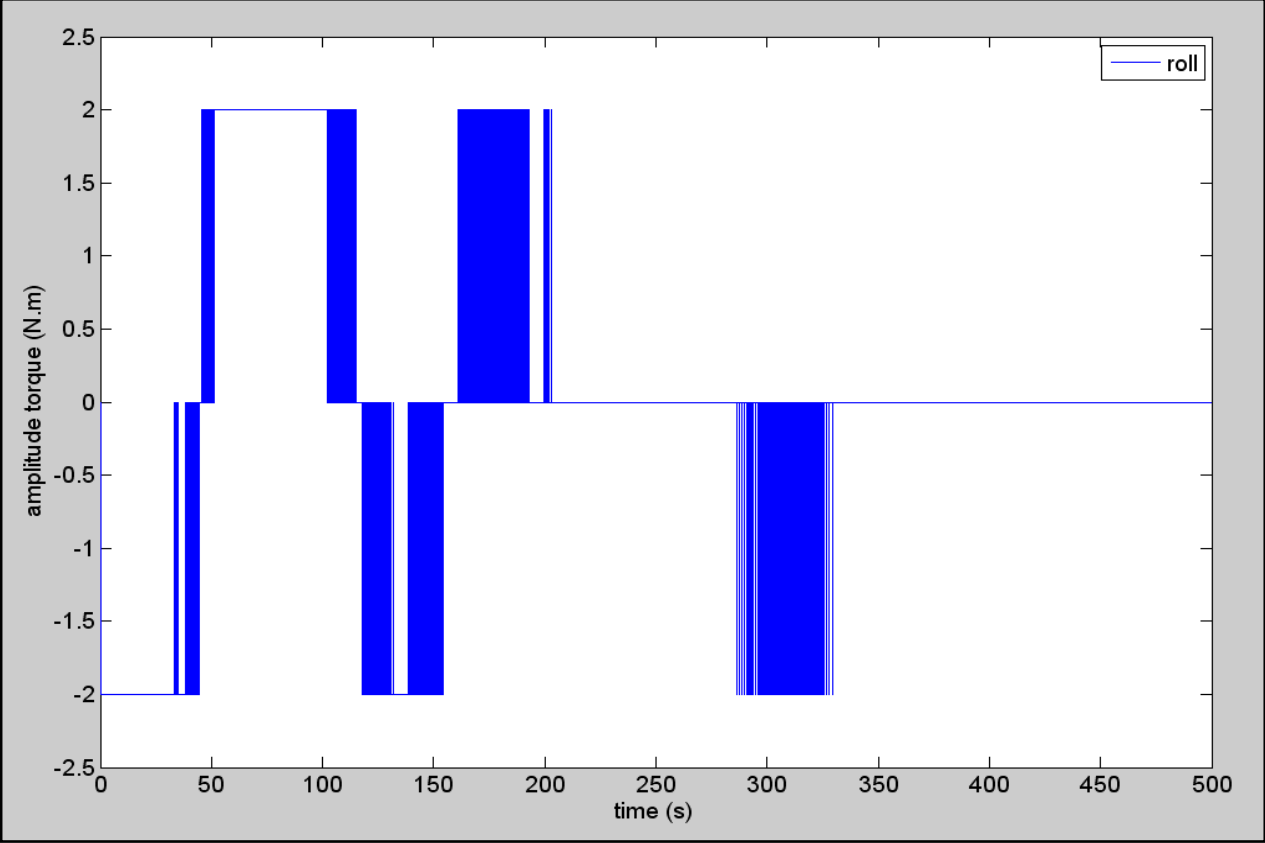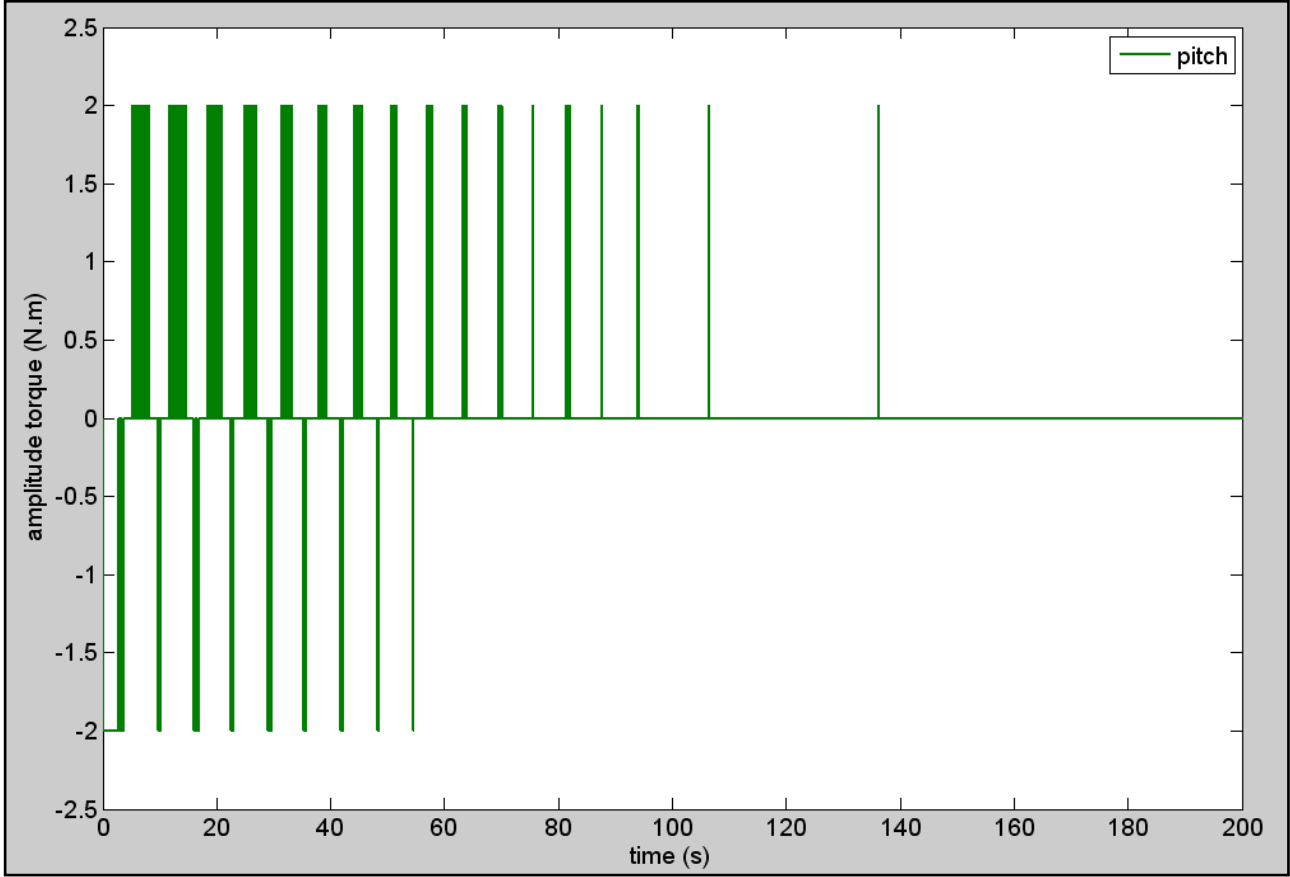

Figure 26 Attitude Maneuvers of the Flexible Satellite using thruster based on PD controller (K= 100, Kd=2000) – amplitude torque of roll angle

In the roll motion, the time for the thruster to stabilize is 346 sec.

Simulation 6: Attitude Maneuvers of the Flexible Satellite using thrusters based on PD controller with **(K= 100, Kd=2000, t=400)** *– amplitude torque of pitch angle*
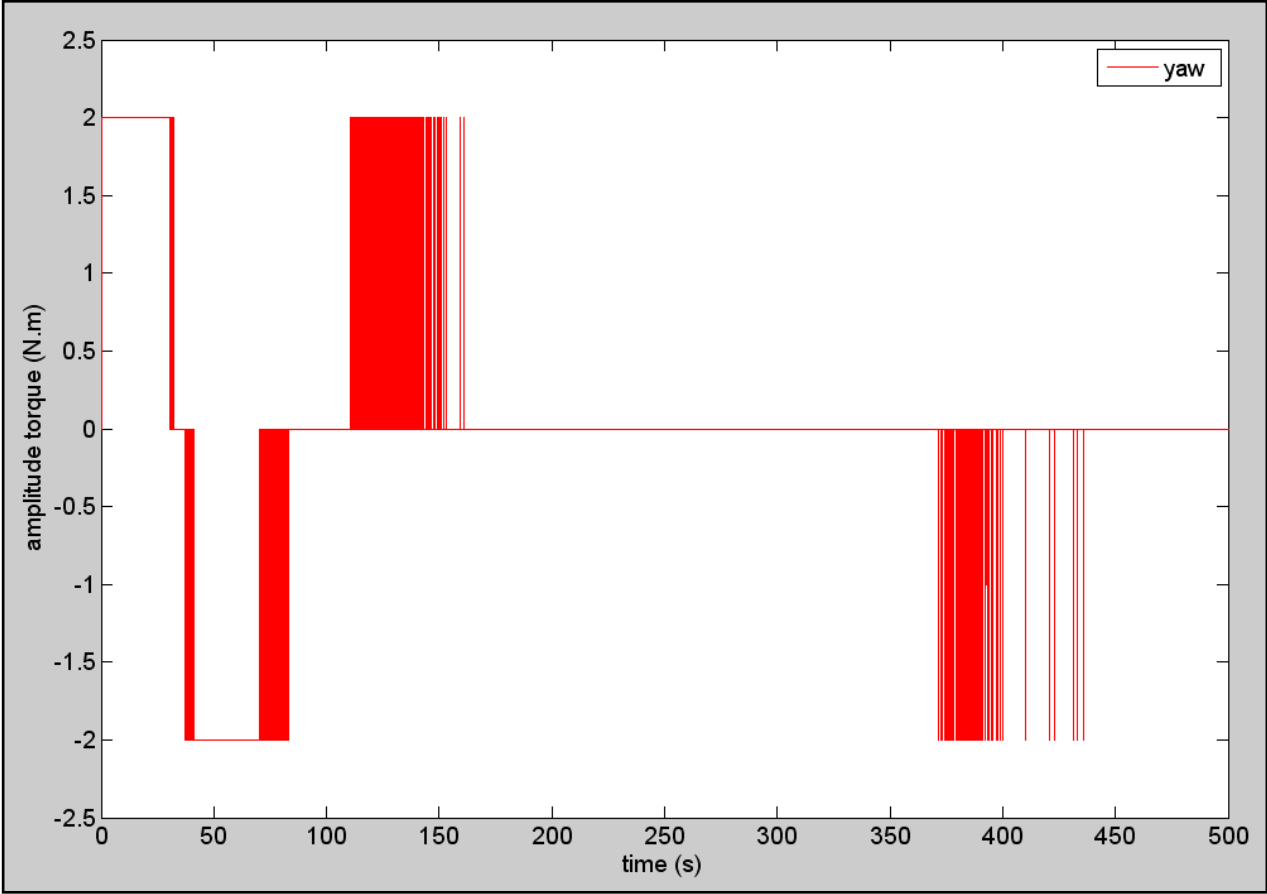

Figure 27 Attitude Maneuvers of the Flexible Satellite using thruster based on PD controller (K= 100, Kd=2000) – amplitude torque of pitch angle

In the pitch motion, the time for the thruster to stabilize is 143 seconds.

Simulation 7: Attitude Maneuvers of the Flexible Satellite using thrusters based on PD controller with **(K= 100, Kd=2000, t=400)** *– amplitude torque of roll angle*

Figure 28 Attitude Maneuvers of the Flexible Satellite using thruster based on PD controller (K= 100, Kd=2000) – amplitude torque of pitch angle

In the yaw motion, the time for the thruster to stabilize is 448 seconds.

Example 6

Another simulation of the thruster amplitude is done using the same parameters but with the different $T_{c\ min.}$ The new value for $T_{c\ min}$ is 0.1 compared to before, is 0.3. The result is observed on the pattern of the thrusters.
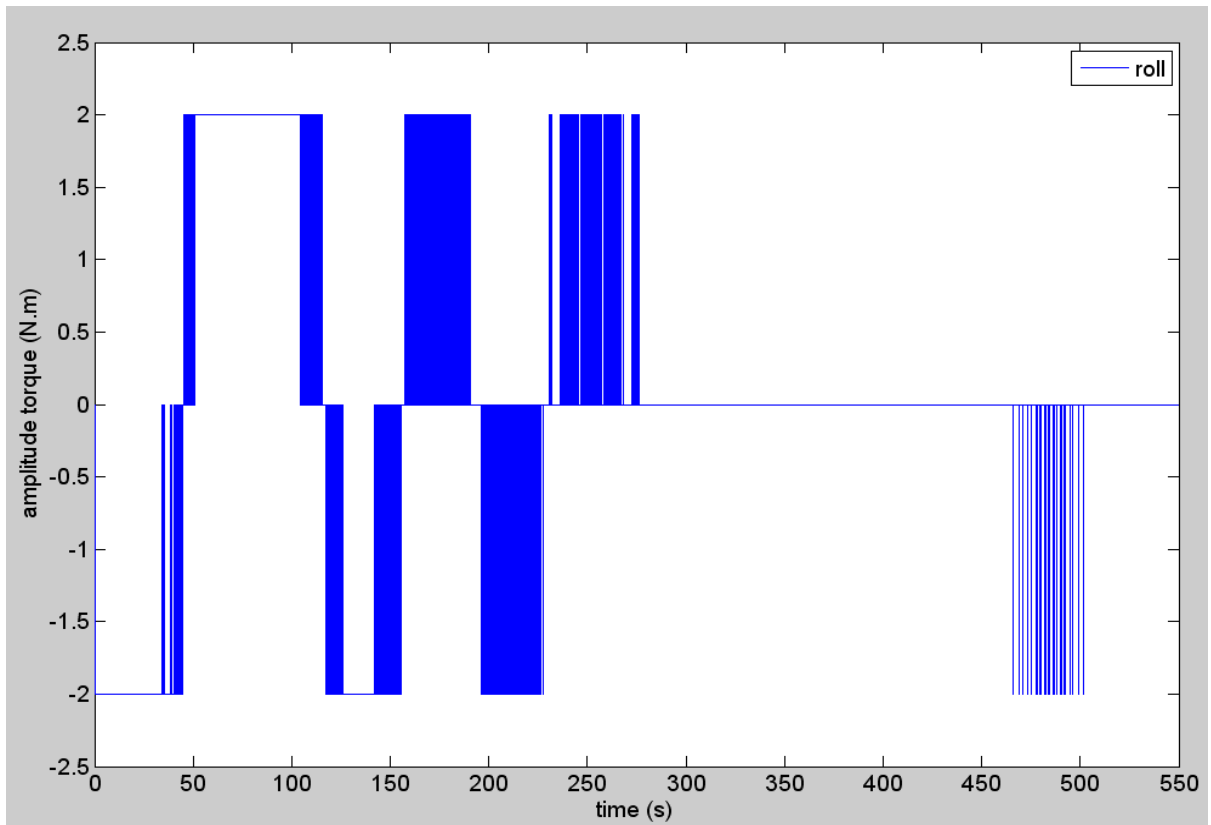

Figure 29 Attitude Maneuvers of the Flexible Satellite using thruster based on PD controller (K= 100, Kd=2000) – amplitude torque of roll angle using $T_{c\ min} = 0.1$

In the roll motion, the time for the thruster to stabilize is 511 sec.

The settling time for the thruster would be longer for the roll and the pitch angle when the $T_{c\ min.}$ is smaller. It is also observed that the changes in the amplitude of thrusters would be more when applying smaller $T_{c\ min.}$.The result for the angle displacement when changing the $T_{c\ min}$ would still be the same.
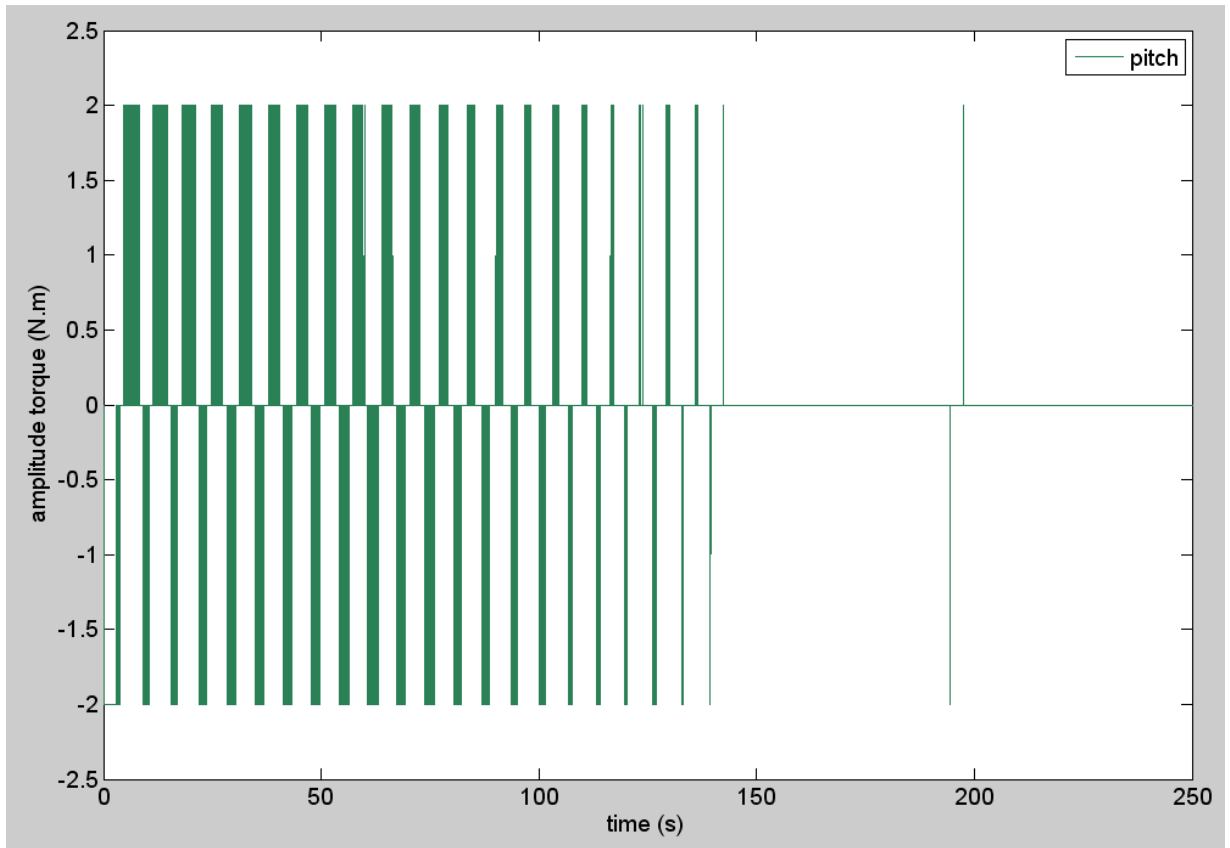
Figure 30 Attitude Maneuvers of the Flexible Satellite using thruster based on PD controller (K= 100, Kd=2000) – amplitude torque of pitch angle using $T_{c\,min} = 0.1$

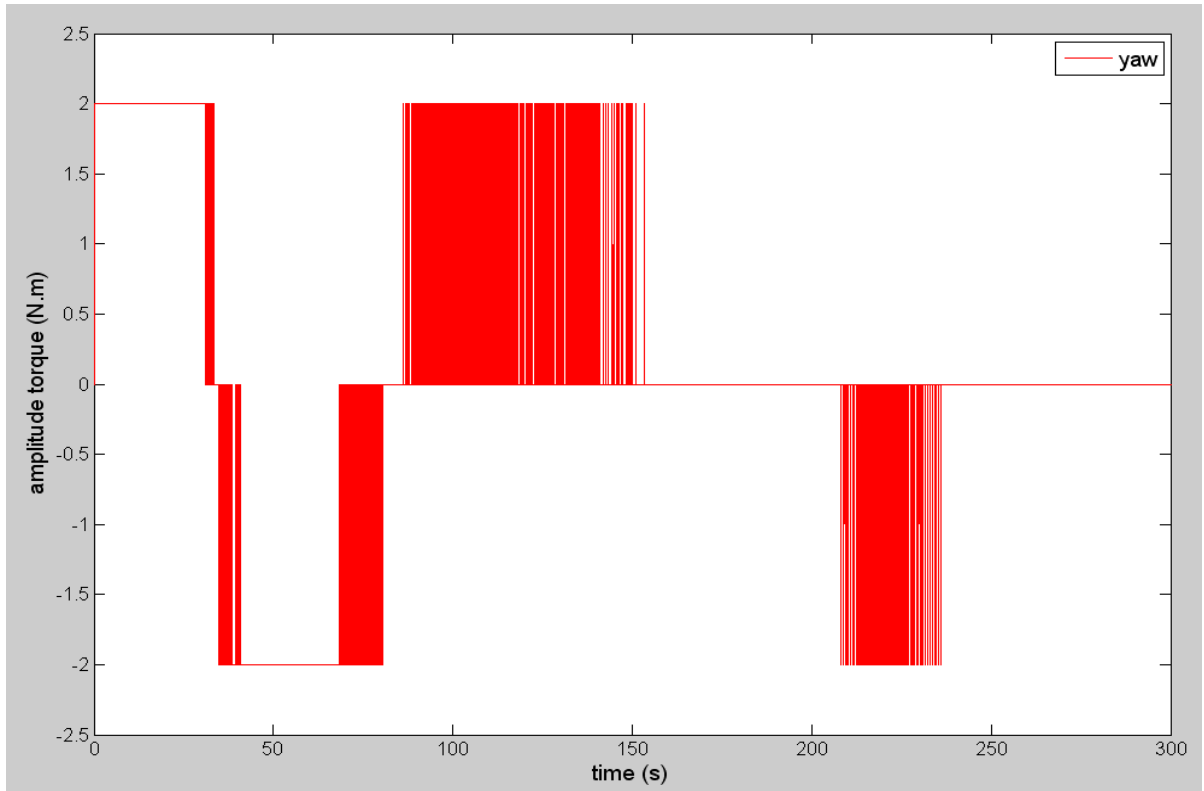Figure 31 Attitude Maneuvers of the Flexible Satellite using thruster based on PD
controller (K= 100, Kd=2000) – amplitude torque of yaw angle using Tc min = 0.1

4.6 DISCUSSION

For Bang-bang control, most of the amplitude of residual roll and yaw angle
oscillate larger compared to the pitch angle. This depends on the natural frequency
excited by the torque of the motion. From the result of the simulation, the residual
oscillation of the roll and the yaw angle are 0.89˚ and 0.47˚, respectively. This would be
very large oscillation compared to our requirement which is less than 0.07˚. Thus, this
kind of oscillation may disturb the satellite's orientation. The settling time for this
controller is faster compared to others, which is less than 100 seconds.

For PD controller, the period of the amplitude of residual pitch angle oscillate
very little compared to the other the angles. This kind of behavior is similar when Bang-
bang controller is used. At some condition, the amplitude of pitch angle may not

55

oscillate at all, **0°**. When few different simulations were done with using different initial angle the period of oscillation for the roll and the yaw angle does not vary much as the initial attitude angle changes. The period of the amplitude are longer compared when using the Bang-bang command control. Most of the simulations done under PD control consume longer response time to achieve stabile state. The steady state errors also are approximately very close to zero, around, 0-0.005˚.

The logic thruster based on PD control was succeeded to maneuver the spacecraft using amplitude thruster in small oscillation after the maneuver. The response time using thruster does not vary much from the PD control, but it still takes longer time to stabilize compared to Bang-bang controller.

In the flexible satellite, the motion of the rigid main body induces vibrations of the flexible substructures, and the vibration of a flexible structural member generates the oscillation of attitude angles of the main body and the vibration of the other flexible structural members. Maneuvering the flexible satellites without regard to its system flexibility will cause a large residual vibration of the flexible modes as well as the residual attitude angle oscillations of the main body. Even though the vibrations of the flexible substructures are cannot be avoided, it can be decrease to certain parameters, with the correct command law.

Vibration reduction is a critical problem related to the maneuvering of modern spacecrafts, which use large, complex, and light weight space structures, such as solar array panels, to achieve increased functionality at a reduced launch cost, but results in the spacecraft being extremely flexible and having low fundamental vibration modes.

CHAPTER 5

CONCLUSION AND RECOMMENDATION

Attitude maneuvers of a flexible satellite using thruster based on the PD controller with constant amplitude torque was successfully simulated. This project is aligned with the plan in the Gantt chart and accomplished in the time range. Other related researches are referred to gain more understanding of the topics. The aim of this report has been achieved.

The possible problem in this work would be for the switching time. The switching time for the thruster has limitation in interval. It cannot be done in very short time interval, for example 0.0015 seconds or 0.015 seconds, etc. For future work, it is recommended that the thruster to be modified so that the time interval should be set to a minimum period of time. It would be impossible to design a thruster by not having any limitations to the on-off jets. If there is a minimum time interval of switching, it is feasible to design the thruster.